A SIMPLE GENERAL EXPRESSION FOR LONGSHORE TRANSPORT OF SAND, GRAVEL AND SHINGLE

by Leo C. van Rijn, The Netherlands; Email: info@leovanrijn-sediment.com,
Website: www.leovanrijn-sediment.com

(published in Coastal Engineering Vol. 90, 2014, 23-39)

1 Introduction

The prediction of reliable estimates of longshore sediment transport is of considerable practical importance in coastal engineering. An example is the evaluation of sediment budgets for coastal areas with and without structures (breakwaters, groynes). Another example is the long-term stability of beach protections and beach nourishments. Most research on longshore transport has concentrated on sand sized sediment, but research on longshore transport along gravel/shingle beaches, which are quite common along mid- and high-latitude (formerly glaciated) parts of the world, has been very limited.

The most widely used formula for longshore transport (LT) is the CERC equation (Shore Protection Manual, US Army Corps of Engineers, 1984). This method is based on the principle that the longshore transport rate (LT, incl. bed load and suspended load) is proportional to longshore wave power P per unit length of beach; LT=K P, with K=calibration coefficient. The CERC formula has been calibrated using field data from sand beaches. The CERC formula does not account for particle size and beach slope. It is only valid for sandy conditions.

The effects of particle diameter and bed slope have been studied systematically by Kamphuis (1991), resulting in a more refined equation for longshore sediment transport. The Kamphuis formula is valid for sand beaches, but is most likely not valid for gravel and shingle beaches. The Kamphuis formula was found to give the best agreement between computed and measured transport rates based on the work of Schoonees and Theron (1993, 1996). Recently Mil-Homens et al. (2013) have made a re-evaluation of the Kamphuis formula based on an extensive set of 250 data points. Most of the data points are in the sand range (<0.6 mm) and low transport range (mild wave conditions). Data sets of gravel and shingle beaches, which is a focus point of the present study, have not been used. The modified Kamphuis 2013 formula will also be used in the present study.

Van Wellen et al. (2000) have evaluated various formulae for coarse-grained beaches, but most of these formulae are not suitable for sand beaches. The formula of Damgaard and Soulsby (1997, 2005) for longshore bed load transport of coarse materials performed rather well. However, this formula does not give the longshore suspended load transport for sand beaches. Tomasicchio et al. (2013) proposed a general set of equations for longshore transport of coarse to fine sediments. They started from available expressions for very coarse materials as used for breakwaters. These expressions were extended to the sand range by a fitting procedure using 245 data points split in various subintervals. An independent verification was not done.

Herein, a detailed process-based model (CROSMOR) has been used to compute the longshore transport rates along sand, gravel and shingle beaches. This model was tested using a small but good-quality field data set (22 data points) of sand and shingle beaches. Then, the model was applied to study the systematic effects of particle size, wave period and profile shape on the longshore transport process. The CROSMOR results have been parameterized and implemented in a new simple formula, which is a modification of the longshore transport formula presented by Van Rijn (2002). The new formula is now dimensionally correct and valid for the size range from sand to shingle and cobbles (0.1 to 100 mm). The effects of additional currents due to tide and wind can be easily included. Short term and long term field and laboratory data have been used for (independent) verification of the new expression.

2 Field data analysis

2.1 Sand beaches

Schoonees and Theron (1993,1996) have made an extensive inventory of the available data sets (about 270) of longshore sand transport rates from a variety of sites around the world. Most data sets refer to mild wave conditions with offshore wave heights smaller than about 2 m and bed material in the sand range of 0.2 to 0.6 mm. The lack of data in the storm range was partly solved by the special storm measurements performed by the US

Army Corps of Engineers (USACE) from the Field Research Facility at the Duck site (USA) in the years of 1995 to 1998 (Miller, 1999). These latter data sets with longshore transport rates in conditions with offshore wave heights up to 4 m have also been used in this study.

Field sites USA	**d_{50} (mm)**	**tanβ (-)**	**$H_{s,br}$ (m)**	**θ_{br} (°)**	**T_p (s)**	**$Q_{t,mass}$ (kg/s)**	**Type of load**
Lake Worth WTTS1 1952	0.42	0.03	0.55	17	7	5	total load
Lake Michigan 1978	0.25	0.08	0.65	25	4	4.3	only suspended
Leadbetter LBB17 1981	0.22	0.046	0.855	6	11	13.5	total load
Leadbetter LBB32 1981	0.22	0.019	1.77	8	11.9	197	total load
Price inlet BU2 1977	0.22	0.018	0.7	9	9.5	7.4	only suspended
Price inlet CA1 1977	0.22	0.027	0.8	9	9.2	16.4	only suspended
Duck, 14 November 95	0.15-0.2	0.025	1.70	10	8	144	only suspended
Duck, 11 March 96	0.15-0.2	0.025	2.40	10	7	483	only suspended
Duck, 27 March 96	0.15-0.2	0.025	1.85	19	7	152	only suspended
Duck, 2 April 96	0.15-0.2	0.025	1.75	19	7	180	only suspended
Duck, 1 April 97	0.15-0.2	0.025	2.85	16	9	395	only suspended
Duck, 19 October 97	0.15-0.2	0.025	3.20	18	10	730	only suspended
Duck, 4 February 98	0.15-0.2	0.025	3.10	19	11	920	only suspended
Duck, 5-7 September 85	0.2	0.025	1.05	3	9.5	4	only suspended
Indian Rocks Run 4 1999	0.35	0.09	0.29	13.4	3.6	0.33	total load
Indian Rocks Run 5 1999	0.35	0.13	0.40	19.7	3.0	0.95	total load

d_{50} = particle size; tanβ= beach/surf zone slope; $H_{s,br}$= significant wave height at breakerline;

θ_{br} = wave angle to shore normal at breakerline; T_p = peak wave period,

Table 1 *Longshore transport data of field sites (sand) in USA*

In the present study 16 reliable data sets (only sand) from 6 sites in the USA have been applied to analyse the longshore sand transport process. All data in the sand range (0.15 to 0.45 mm) were taken from the original data reports and papers and checked for reliability. The data sets from Duck (USA) and Indian Rocks (USA) were taken because they represent the two extreme ends (high breaking waves up to 3.2 m and low waves of 0.3 m) of the transport range. The other data sets are in the intermediate transport range (waves in the range of 0.5 to 2 m), see Table 1.

All data sets satisfy the criteria of available wave conditions (height, period and angle), transport rates, beach slopes and grain sizes. Most data sets used herein refer to short-term measurements using direct sampling methods or short-term volume changes at USA field sites. As regards long-term volume changes, only one case with a predominant wave direction has been considered (Leadbetter Beach, USA). Most often, the longshore transport rates are given as bulk volumetric rates ($Q_{t,volume}$ in m^3 per day). This value has been converted to the mass transport rate ($Q_{t,mass}$ in kg/s) by using $Q_{t,mass}$= (1-p) ρ_s $Q_{t,volume}$ with p= porosity factor (0.4 for sand and 0.45 for shingle) and ρ_s= sediment density (=2650 kg/m^3). The measured transport rates are in a very wide range of 0.3 to 900 kg/s (factor 3000 !).

The characteristics of the 6 field sites are:

- **South Lake Worth, Florida, USA (1953)**; low wave and microtidal conditions (swell); medium coarse sand bed of 0.4 to 0.6 mm; data based on bypassing rate of sand pumping plant (Watts, 1953);
- **Leadbetter Beach, California, USA (1981)**; mild wave conditions (swell); fine sand of 0.2 to 0.25 mm; data based on morphological volume changes along beach over about 1 year (Gable, 1981);
- **Lake Michigan, Wisconsin, USA (1975)**; low wave energy conditions; medium fine sand of 0.2 to 0.3 mm; data based on trap samplers (Lee, 1975);
- **Price Inlet, South Carolina, USA (1977)**; low wave energy conditions (swell); medium fine sand of 0.2 to 0.25 mm; data based on trap samplers (Kana et al., 1977; Kana and Ward, 1980);
- **Indian Rocks beach, Florida, USA (1999)**; very low wave-energy and microtidal conditions; medium coarse sand bed of 0.35 mm; data based on short-term morphological volume changes (<1 day) (Wang and Kraus, 1999);
- **Duck site, USA (1985 and 1995-1998)**; medium to high waves and microtidal conditions; fine sand bed of 0.15 to 0.2 mm; data based on sampling using streamer traps during swell conditions in September 1985 (Kraus and Dean, 1987); electronic concentration sampling during storm conditions (Miller, 1999).

This relatively small but reasonably good-quality data set was used to establish the relationship between wave height, wave incidence angle and longshore transport. It is realized that the applied sand data set is small, but in section 3.2 it will be shown that this data set actually is quite representative. More data of the same will give more scatter, but this may help to better define the envelope of variation in the data.

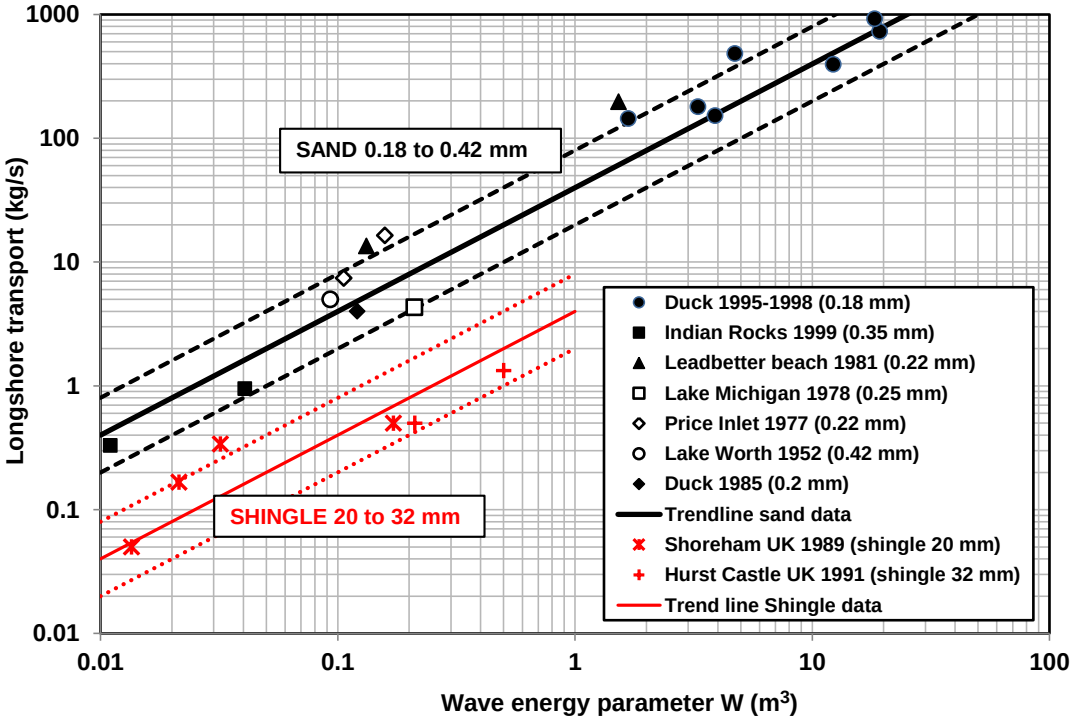

Figure 1 *Longshore sediment transport (sand, shingle) as function of wave energy parameter* $W = (H_{s,br})^3 \sin(2\theta_{br})$

The measured total longshore sand transport rates (16 cases from 6 field sites) are plotted in Figure 1 as function of the parameter $W = (H_{s,br})^3 \sin(2\theta_{br})$. The power of the wave height is found to be about 3 based on two extreme cases with very low waves (Indian Rocks site) and high waves (Duck site). Most transport rates are within a factor of 2 of the plotted trend line.

The trend line can be represented by (see also Van Rijn, 2002):

$$Q_{t,mass} = K_{sand} (H_{s,br})^3 \sin(2\theta_{br}) \quad (1)$$

with: $Q_{t,mass}$ = longshore sand transport (in kg/s; dry mass); $H_{s,br}$ = significant wave height at breakerline (in m); θ_{br} = wave incidence angle (to shore normal) at breakerline (degrees) and K_{sand}= 40 (kg/s/m^3).
Equation (1) is valid for sand in the range of 0.15 to 0.42 mm and beach slopes in the range of 0.02 to 0.1. The complete data set for sand is too small to detect any influence of particle size and/or beach slope

2.2 Gravel and shingle beaches

Longshore transport data of shingle beaches (sizes of 15 to 30 mm) are extremely scarce. The main reason for the lack of reliable field data is the lack of robust instrumentation to measure the hydrodynamics and the transport rates at shingle beaches (Van Wellen et al., 2000). Most often, tracers are used but major problems are the poor recovery rates and the estimation of the depth of the moving layer. Traps also have serious drawbacks in that they are difficult to deploy and interfere with the flow field and easily develop scour holes. Reliable estimates require the presence of shore-normal barriers (groynes) which will block the longshore transport rate (impoundment method) in conditions with one dominant wave direction.
Only two field data sets satisfy the criteria of available wave conditions (height, period and angle), transport rates, beach slopes and grain sizes. These two field sites are: Shoreham-by-Sea in west Sussex of the UK (Chadwick, 1989) and Hurst Castle Spit in the UK (Nicholls and Wright, 1991).

- Shoreham UK (1989); low waves in macro-tidal conditions; prevailing wave direction is from south-west (English Channel); shingle of 20 mm; beach slope of 1 to 8; measured by traps;
- Hurst Castle Spit UK (1991); low to medium waves in meso-tidal conditions; prevailing wave direction is from south-west (English Channel); shingle of 16 to 32 mm; beach slope of 1 to 10; measured by tracers.

The basic shingle data are given in **Table 2**.

Field sites UK	**d_{50} (mm)**	**tanβ (-)**	**$H_{s,br}$ (m)**	**θ_{br} (^{o})**	**T_p (s)**	**$Q_{t,mass}$ (kg/s)**	**Type of load**
Shoreham UK 1989	20	0.1	0.3	15	3	0.05	bed load
	20	0.1	0.35	15	3	0.167	bed load
	20	0.1	0.4	15	3	0.3	bed load
	20	0.1	0.7	15	4	0.5	bed load
Hurst Castle Spit UK 1991	32	0.1	0.75	15	6	0.5	bed load
	32	0.1	1.0	15	6	1.5	bed load

d_{50} = particle size; tanβ = beach slope, $H_{s,br}$= significant wave height at breakerline,
θ_{br} = wave angle to shore normal at breakerline, T_p = peak wave period,

Table 2 *Longshore transport data of field sites (shingle) in UK*

The longshore transport rates (6 data points) of shingle are also shown in Figure 1. The trendline can also be represented by Equation (1) with $K_{shingle}$= 4 (kg/s/m^3). Most data points are within a factor of 2 of the trendline. Comparing both trendlines (sand and shingle), it is found that the shingle transport rates are much smaller (about

factor 10) than the sand transport rates. Assuming a mean sand size of 0.3 mm and a mean shingle size of 30 mm (factor 100 larger), the longshore transport rate (LT) is roughly proportional to the root of $1/d_{50}$ or $LT \approx (d_{50})^{-0.5}$. The complete data set of 22 points is however, much too small to unveil the proper effect of grain size and possibly the effect of beach/surf zone slope on the longshore transport rate. To study these effects properly, the detailed CROSMOR-model has been used.

3 Longshore transport based on detailed cross-shore model

3.1 Model description

A detailed process-based model (CROSMOR2013) has been used in this study to compute the longshore sediment transport distribution along the cross-shore bed profile. First, this model was tested using the available field data sets. Then, the model was applied to study the systematic effects of particle size, wave period and profile shape on the longshore transport process.

The CROSMOR model comprises three submodules: hydrodynamics (waves, currents), sand transport and bed level evolution (morphology). The CROSMOR2013-model is an updated version of the CROSMOR2004-model (Van Rijn 2006/2012, 2007d) and computes both the cross-shore and longshore transport rates. The model has been extensively validated by Van Rijn et al. (2003) and Van Rijn et al. (2011).

The propagation and transformation of individual waves (wave by wave approach) along the cross-shore profile is described by a probabilistic model (Van Rijn and Wijnberg, 1994, 1996) solving the wave energy equation for each individual wave. The individual waves shoal until an empirical criterion for breaking is satisfied. The maximum wave height is given by $H_{max}=\gamma_{br}$ h with γ_{br}= breaking coefficient and h=local water depth. The default wave breaking coefficient is represented as a function of local wave steepness and bottom slope. The default breaking coefficient varies between 0.4 for a horizontal bottom and 0.8 for a very steep sloping bottom. The model can also be run a with a constant breaking coefficient (input value). Wave height decay after breaking is modelled by using an energy dissipation method. Wave-induced set-up, set-down and breaking-associated longshore currents are also modelled. Laboratory and field data have been used to calibrate and to verify the model. Generally, the measured $H_{1/3}$-wave heights are reasonably well represented by the model in all zones from deep water to the shallow surf zone. The fraction of breaking waves is reasonably well represented by the model in the upsloping zones of the bottom profile. Verification of the model results with respect to wave-induced longshore current velocities has shown reasonably good results for barred and non-barred profiles (Van Rijn et al., 2003; Van Rijn and Wijnberg, 1994, 1996).

The complicated cross-shore wave mechanics in the swash zone near the water line is not explicitly modelled, but taken into account in a schematized way (see Van Rijn and Sutherland, 2011). The limiting water depth of the last (process) grid point is set by the user of the model (input parameter; typical values of 0.1 m). Based on the input value, the model determines the last grid point by interpolation after each time step (variable number of grid points). The process-based model parameters are computed up to the last grid point.

The cross-shore wave velocity asymmetry under shoaling and breaking waves is described by the semi-empirical method of Isobe and Horikawa (1982) with modified coefficients (Grasmeijer and Van Rijn, 1998; Grasmeijer ,2002) or by the recently proposed method of Ruessink et al. (2012). Near-bed streaming effects are modelled by semi-empirical expressions based on the work of Davies and Villaret (1997, 1998, 1999). The velocity due to low-frequency waves in the swash zone is also taken into account by an empirical method.

The depth-averaged return current (u_r) under the wave trough of each individual wave (summation over wave classes) is derived from linear mass transport and the water depth (h_t) under the trough. The mass transport is given by $0.125\ g\ H^2/C$ with H=wave height and $C=(g\ h)^{0.5}$ = phase velocity in shallow water. The contribution of the rollers of broken waves to the mass transport and to the generation of longshore currents (Svendsen, 1984; Dally and Osiecki, 1994) is taken into account.

The sand transport of the CROSMOR2013-model is based on the TRANSPOR2004 sand transport formulations (Van Rijn, 1993/2006, 2007a,b,c,d). The effect of the local cross-shore bed slope on the transport rate is taken into account. The sand transport rate is determined for each wave (or wave class), based on the computed wave height,

depth-averaged cross-shore and longshore velocities, orbital velocities, friction factors and sediment parameters. The net (averaged over the wave period) total sediment transport is obtained as the sum of the net bed load (q_b) and net suspended load (q_s) transport rates. The net bed-load transport rate is obtained by time-averaging (over the wave period) of the instantaneous transport rate using a formula-type of approach.
The net suspended load transport is obtained as the sum ($q_s = q_{s,c} + q_{s,w}$) of the current-related and the wave-related suspended transport components. The current-related suspended load transport ($q_{s,c}$) is defined as the transport of sediment particles by the time-averaged (mean) current velocities (longshore currents, rip currents, undertow currents). The wave-related suspended sediment transport ($q_{s,w}$) is defined as the transport of suspended sediment particles by the oscillating fluid components (cross-shore orbital motion). The oscillatory or wave-related suspended load transport ($q_{s,w}$) has been implemented in the model, using the approach of Houwman and Ruessink (1996). The method is described by Van Rijn (2007a,b,c,d). Computation of the wave-related and current-related suspended load transport components requires information of the time-averaged current velocity profile and sediment concentration profile. The convection-diffusion equation is applied to compute the time-averaged sediment concentration profile based on current-related and wave-related mixing. The bed-boundary condition is applied as a prescribed reference concentration based on the time-averaged bed-shear stress due to current and wave conditions. It is noted that the sediment transport in the uprush zone beyond the mean water line is neglected. This will lead to underprediction of the longshore gravel/shingle transport for very low, oblique waves (< 0.5 m) when the swash-type transport is dominant. This is of less importance for higher waves (>1 m) when the longshore transport in the inner surf zone is dominant.

3.2 Model verification for sand beaches

The CROSMOR model has been used to compute the longshore transport rate (bed load plus suspended load) of the 16 field data sets (sand) of **Table 1**. The wave parameters are known at the breakerline, see **Table 1**. The breakerline of the probabilistic CROSMOR-model is defined at the location where approximately 5% of the waves are breaking (the percentage of breaking waves is an output result of the CROSMOR-model). During storm conditions with high waves (> 3 m) the breakerline is close to the 8 m depth contour. The model input was iteratively changed until the results at the model breakerline were identical to the measured values of each case of **Table 1**. Each case was represented by 10 wave classes assuming a Rayleigh-distribution with $H_{1/3}$ being equal to the measured value. The wave-related and current-related bed roughness values ($k_{s,w}$ and $k_{s,c}$) were varied in the range of 0.01 to 0.03 m to evaluate the uncertainty range (about 20% to 30%) of the computed longshore transport values.
Figure 2 shows typical results of the computed cross-shore distributions of significant wave height, longshore current velocity and longshore suspended flux for one of the field cases: storm event 2 April 1996 at the Duck site (USA), see **Table 1**. The computed wave heights are somewhat too small above the breaker bar in the inner surf zone. The computed longshore current velocities are reasonably well represented. The model produces a longshore velocity distribution with peaks above the breaker bar and near the water line in agreement with the observed values. The computed longshore suspended sand transport rates are in reasonable agreement with measured values in the outer surf zone, but the computed values are too small (factor 2) in the inner surf zone. The longshore bed load transport was not measured.
The computed longshore sand transport rates (bed load plus suspended load) for all 16 cases of Table 1 based on the CROSMOR-model are shown in **Figure 3**. Two other methods have also been used: the CERC-method and the Kamphuis 1991-method.
The CERC-formula developed by the US-Corps of Engineers relates the immersed weight (I) of the longshore sediment transport rate to the longshore wave energy flux factor (Shore Protection Manual, 1984):

This formula can be rearranged into (Van Rijn, 1993,2006):

$$Q_{t,mass} = 0.023\,(1-p)\,\rho_s\,g^{0.5}\,(\gamma_{br})^{-0.51}\,(H_{s,br})^{2.5}\,\sin(2\theta_{br}) \qquad (2)$$

Equation (2) is dimensionally correct. Using p= porosity=0.4 , ρ_s = 2650 kg/m^3 and γ_{br}= breaking coefficient = 0.8:

$$Q_{t,mass} = 128\ (H_{s,br})^{2.5} \sin(2\theta_{br}) \qquad (3)$$

with: $Q_{t,mass}$= longshore transport rate (dry mass, in kg/s), $H_{s,br}$= significant wave height at breaker line; θ_{br} = wave angle at breaker line (between wave crest line and coastline; or between wave propagation direction and shore normal direction). The coefficient 128 has dimensions and $H_{s,br}$ is in metres. The most important parameters are the wave height and the wave angle. Equation (2) is a rather crude formula, not showing any influence of the particle diameter and the beach/surf zone slope. Therefore, the CERC-formula is only valid for a narrow range of conditions as represented by the calibration data. The formula is most valid for sandy ocean coasts.

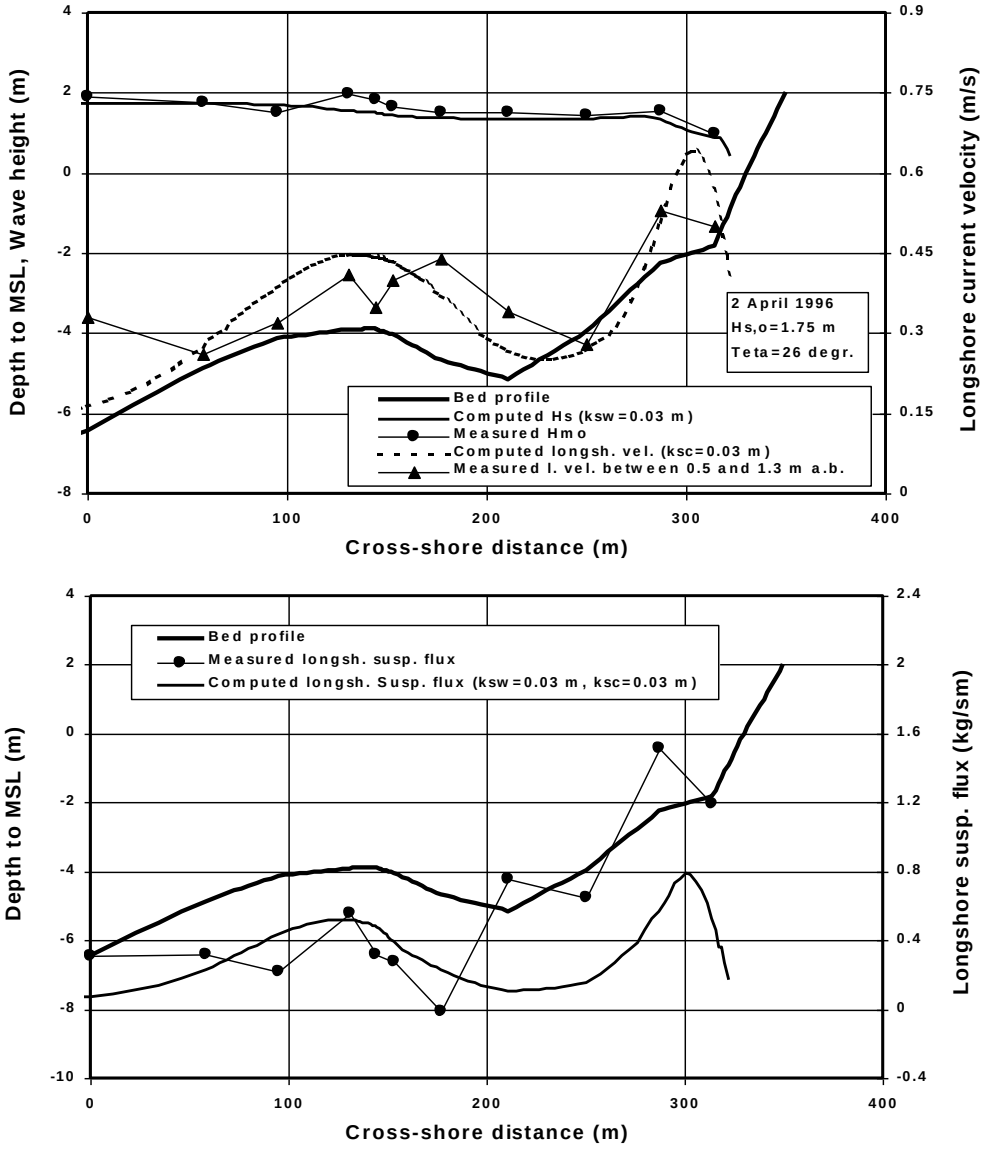

Figure 2 *Wave height, longshore current velocity and sand transport along cross-shore profile of Duck site, 2 April 1996; d_{50}=0.15-0.2 mm (a.b.=above bed)*

The Kamphuis (1991) method is given by:

$$Q_{t,mass}=2.33\ \rho_s/(\rho_s-\rho)\ (T_p)^{1.5}\ (\tan\beta)^{0.75}\ (d_{50})^{-0.25}\ (H_{s,br})^2\ [\sin(2\theta_{br})]^{0.6} \qquad (4a)$$

with: $Q_{t,mass}$= longshore sediment (dry mass in kg/s); $H_{s,br}$=significant wave height at breaker line (m); θ_{br} =wave angle at breaker line (°); d_{50}=median particle size in surf zone (m); tan β= beach slope; T_p = peak wave period, p= porosity factor (=0.4). Equation (4a) is dimensionally not correct.
The modified Kamphuis (Mil-Homens et al., 2013) method is given by:

$$Q_{t,mass}=0.15\ \rho_s/(\rho_s-\rho)\ (T_p)^{0.89}\ (\tan\beta)^{0.86}\ (d_{50})^{-0.69}\ (H_{s,br})^{2.75}\ [\sin(2\theta_{br})]^{0.5} \qquad (4b)$$

It is noted that the modified Kamphuis formula given by Mil-Homens et al. (2013) contains two errors (Personal Communication). Equation (4b) is the correct one.

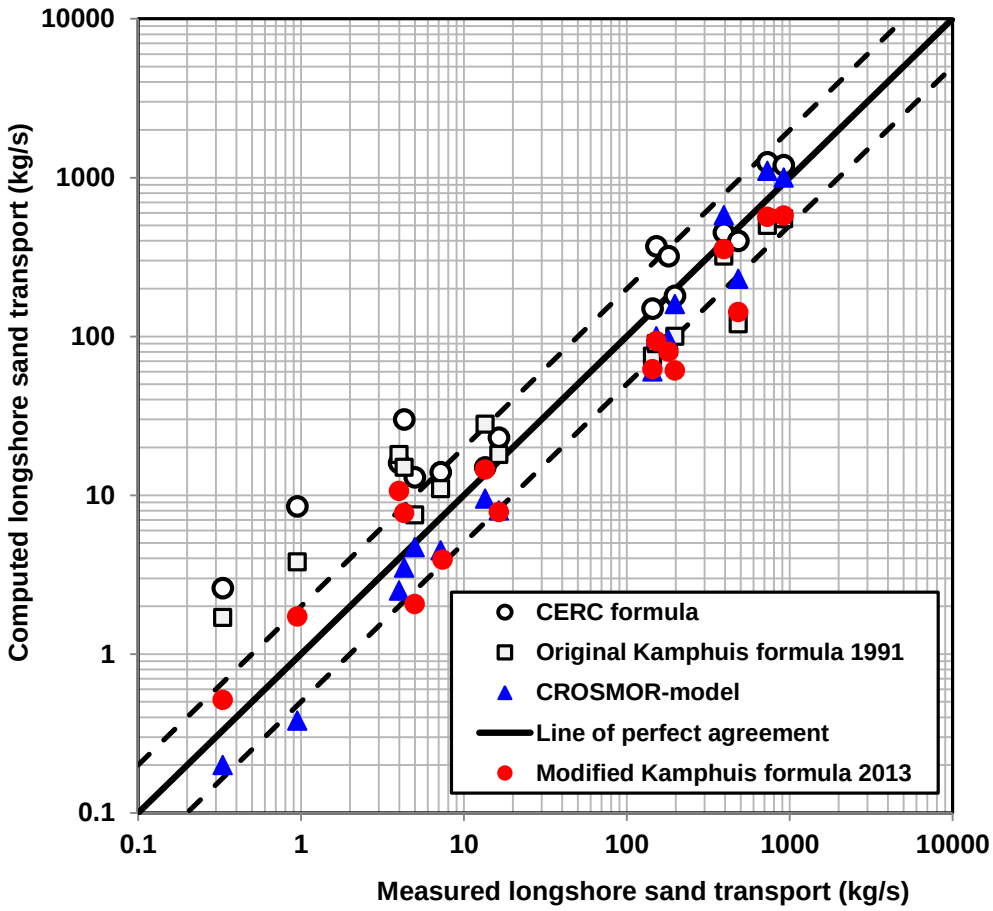

Figure 3 *Comparison of measured and computed longshore transport rates; sand beaches (0.15-0.42 mm)*

The CROSMOR model yields results (see **Figure 3**), which are slightly too large (factor 1.5) for storm conditions (high energy events) and somewhat too small (factor 2) for low wave conditions. It is found that the longshore transport rates during swell conditions are much better simulated using a regular wave train instead of an irregular wave train. The underprediction of the CROSMOR-model for low wave conditions is most likely related to the neglect of the longshore transport in the uprush zone, which is relatively important for low wave conditions. The CROSMOR

model yields reasonably good results using a wave-related ($k_{s,w}$) bed roughness of about 0.03 m for all cases considered. The current-related ($k_{s,c}$) bed roughness is in the the range of 0.01 to 0.03 m. These values are representative for washed-out and developed rippled beds. The bed roughness was used as a tuning parameter of the CROSMOR-model to obtain good predictions over the whole transport range (0.1 to 1000 kg/s).

The CERC and Kamphuis formulae have been used to evaluate their behaviour over the large transport range. The CERC formula yields results, which are slightly too large (factor 2) for storm conditions (high energy events), but much too large (factor 10) for low wave conditions. The original Kamphuis 1991 formula yields results, which are slightly too small (factor 1.5) for storm conditions (high energy events) but too large (factor 4) for low wave conditions. This behaviour is caused by the second power relationship between transport and wave height. The modified Kamphuis 2013 formula yields much better results. The strong overprediction for low waves is absent now. About 60% of the predicted transport rates of the modified Kamphuis formula are within a factor of 2 of the measured values. This score for 16 data points is about equal to the score of the modified Kamphuis formula reported by Mil-Homens et al. for about 250 data points. This confirms that the relatively small sand data set (16 data points) used in this study is quite representative. Furthermore, the Figure 8 of Mil-Homens et al. shows that the modified Kamphuis formula still overpredicts slightly for low waves and underpredicts for high waves, similar to the results of **Figure 3** of this study.

3.3 Model verification for shingle beaches

Coarse-grained gravel and shingle beaches are characterised by rather steep slopes, often interrupted by berms and swash bars. Gravel and shingle grains on beaches are moved almost exclusively by wave action (asymmetric wave motion); tidal or other currents are not effective in moving gravel/shingle material. The coarse grains move up the beach to the run-up limit by strong bores (uprush) and move down the beach close to the line of the steepest beach slope by the backwash (less strong due to percolation) plus gravity, resulting in a saw-tooth (zig-zag) movement in the presence of wave-induced longshore currents. Long-period swell waves on steep beaches can produce relatively large swash velocities up to 3 m/s to move the coarse grains as intensive bed load along the beach face.
To justify that the CROSMOR-model produces realistic results for steep gravel beaches, various verification cases are shown: 1) the reshaping of beach profiles under cross-shore waves for a laboratory experiment and for Pevensey Bay (UK) and 2) the computation of the longshore transport rate of shingle for the field sites of Shoreham and Hurst Castle (UK).
Van Rijn and Sutherland (2011) have applied the process-based CROSMOR-model and the empirical parametric SHINGLE-model of HR Wallingford to simulate the erosion of gravel and shingle barriers under high wave conditions (storm events). Test results of the Deltaflume and Grossen Wellen Kanal (GWK) have been used to calibrate the CROSMOR-model for gravel and shingle slopes. Qualitatively the results are in reasonable agreement with the measured values. **Figure 4** shows computed and measured beach profiles for an experiment in the Grossen Wellen Kanal (GWK) in Hannover, Germany (Van Rijn, 2009). Both models produce a clear swash bar of the right order of magnitude at the upper beach.

Figure 5 shows computed profiles of the shingle beach at Pevensey Bay (UK) for a storm event with an offshore wave height of 6 m. The results of the CROSMOR-model and the empirical SHINGLE-model show rather good agreement. Finally, the CROSMOR-model has been used to compute the longshore transport rate of shingle for the 6 data points of **Table 2**. The bed roughness values are taken equal to the median grain sizes, see **Table 2**. **Figure 6** shows the measured and computed transport rates as function of the wave height at Shoreham and Hurst Castle (UK). The model predictions for the lowest wave heights (0.3 to 0.4 m) are much too small (factor 2 to 3). The model predictions for the highest wave heights (0.7 to 1 m) are about 50% too small. The main reason for the significant underprediction in the case of very low waves is the neglect of the longshore transport in the uprush zone above the mean waterline. This uprush zone above the waterline is not included in the CROSMOR-model. For higher wave conditions (storms) the neglect of the transport in the uprush zone is of minor importance, as the surf zone with breaking waves is much wider than the swash zone. The methods of CERC and Kamphuis (1991) have also been used

for these cases (not shown). The computed values are much too large, which is expected as both methods are not really valid for shingle beaches.
Based on the results of Figures 4 to 6, it is concluded that the CROSMOR-model is able to simulate the cross-shore and longshore transport processes at shingle beaches with reasonable accuracy except for low wave conditions (<0.5 m).

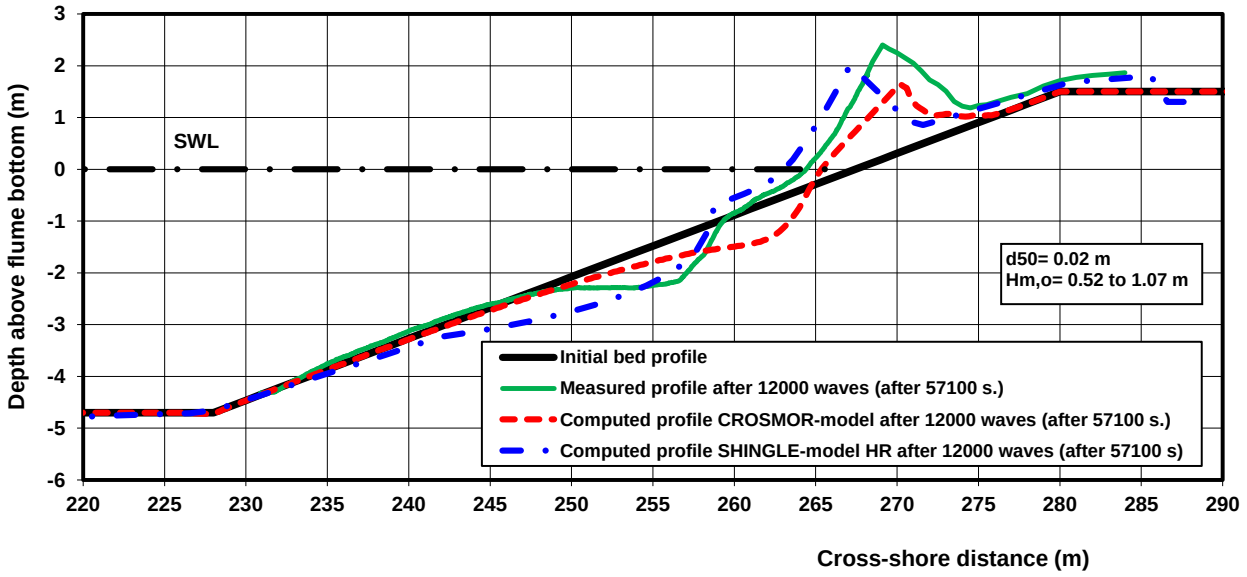

Figure 4 *Simulation of GWK Germany Test 1 to 5 ($H_{m,o}$= 0.52 to 1.07 m; d_{50}=0.02 m)*

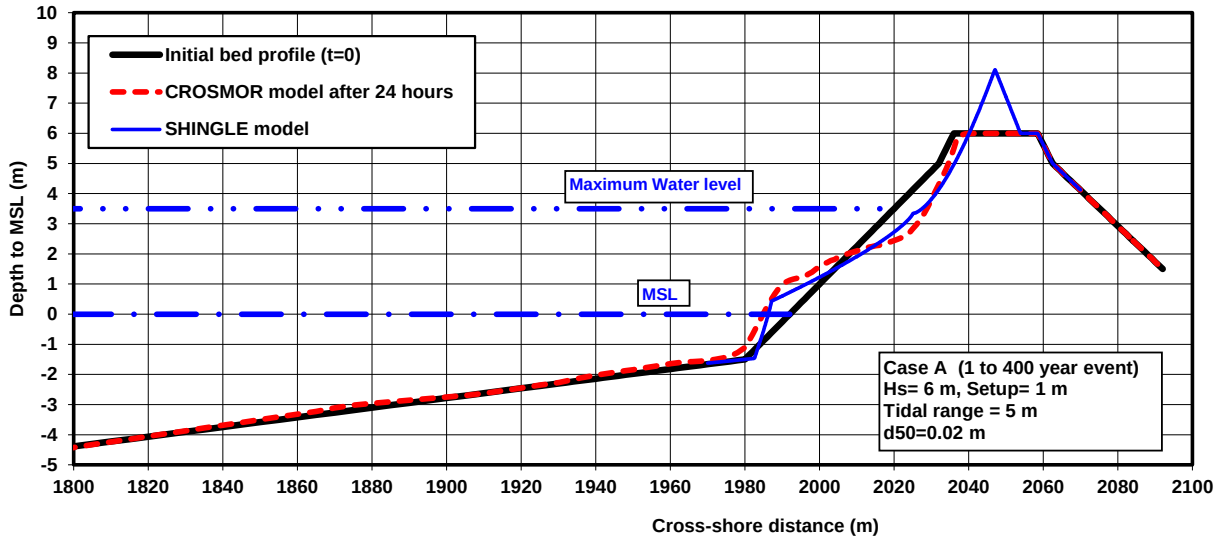

Figure 5 *Computed bed profiles of CROSMOR and SHINGLE models for Pevensey Bay ($H_{s,o}$ = 6 m; d_{50}=0.02 m)*

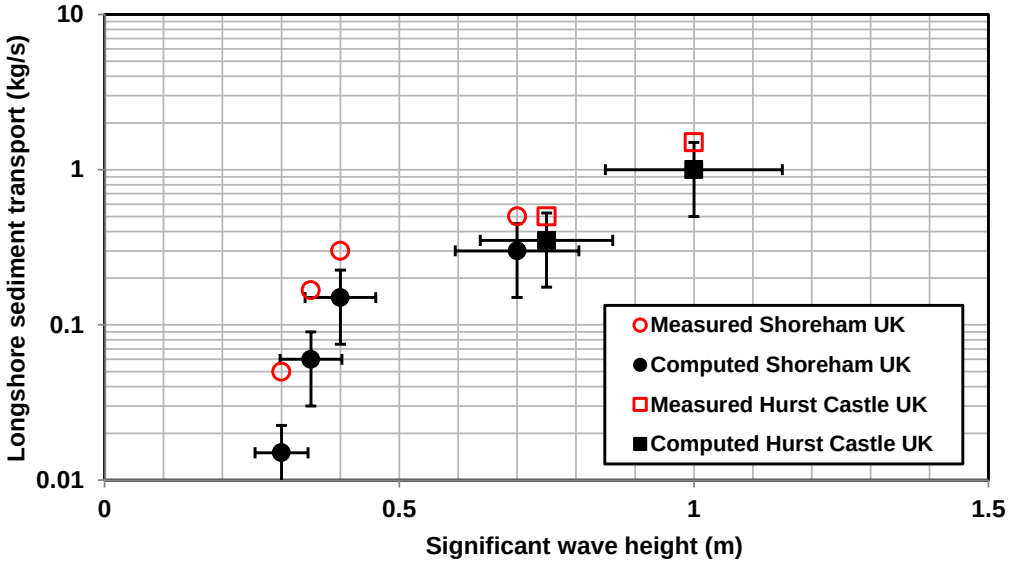

Figure 6 *Measured and computed longshore transport rates of shingle (Shoreham and Hurst Castle, UK)*

3.4 Effect of key parameters on longshore transport based on CROSMOR-model

The model verification study has shown that the process-based CROSMOR-model yields reasonable results for sand and shingle beaches provided that the waves are not very low (<0.5 m). The CROSMOR-model will now be used to study the effects of various key parameters such as wave period, grain size, beach/surf zone slope and the type of waves (regular swell waves or irregular wind waves). It is noted that the CROSMOR model results will only be used in relative sense to find the effect of the key parameters. Furthermore, only cases with waves larger than 1 m will be used. The computed longshore transport rates will be normalized using reference values. In all cases the bed roughness was assumed to be constant along the cross-shore profile and varied in the range of 0.02 to 0.05 m (input value).

3.4.1 Effect of swell waves (wave period)

For wind waves the wave period normally increases with increasing wave height from about 5 s for a wave height of 1 m to about 15 s for offshore wave heights of about 5 m. To assess the influence of the wave period for a constant wave height, some sensitivity computations have been made for a smaller and larger wave period (with constant wave height). An increase or decrease of the wave period of about 20% at the same wave height (in the range of 1 to 5 m) was found to give a similar increase/decrease of the maximum longshore current velocity and sand transport (almost linear effect). Thus, if the wave period is underestimated by maximum 20%, the longshore transport will also be underestimated by maximum 20%. Based on this, it is concluded that the wave period of irregular wind waves is not really a key parameter for longshore transport. Thus, it is not so important if the inaccuracy of the wave period is of the order of 20%.

Low swell waves of 1 to 2 m high generally have a relatively large wave period in the range of 10 to 20 s. Furthermore, swell waves are more regular than wind waves. The influence of swell waves on the longshore transport has been studied by comparing the longshore transport for irregular wind waves of H_{rms}= 1 m and T_p= 7 s with that of regular swell waves of the same wave height H=1 m but with twice the wave period T= 14 s. The irregular wind waves were assumed to have a Rayleigh-type wave height distribution (represented by 10 wave classes with wave heights between 0.5 and 2 m). The offshore wave angle was assumed to be 30 degrees. The grain sizes were in the range of 0.2 to 50 mm. The bed roughness values were varied in the range of 0.02 to 0.05 m (input values). The beach slope was 1 to 30 and 1 to 60 between -1 m and +3 m for grain sizes smaller than 2 mm and 1 to 10 and 1 to 20 for larger grain sizes. The surf zone slope was 1 to 60 between -6 m and -1 m. The sea bed slope between -6 and -20 m was 1 to 200. The swell effect is defined as the ratio $K_{swell}= Q_{t,swell}/Q_{t,ww}$ with $Q_{t,swell}$= longshore

transport due to regular swell waves ($H=H_{rms}$, $T=2T_p$) and $Q_{t,ww}$= longshore transport due to irregular wind waves of the the same wave height (H_{rms},T_p). The computations have been repeated for $H=H_{rms}$=2 m and $T=2T_p$= 16 s).

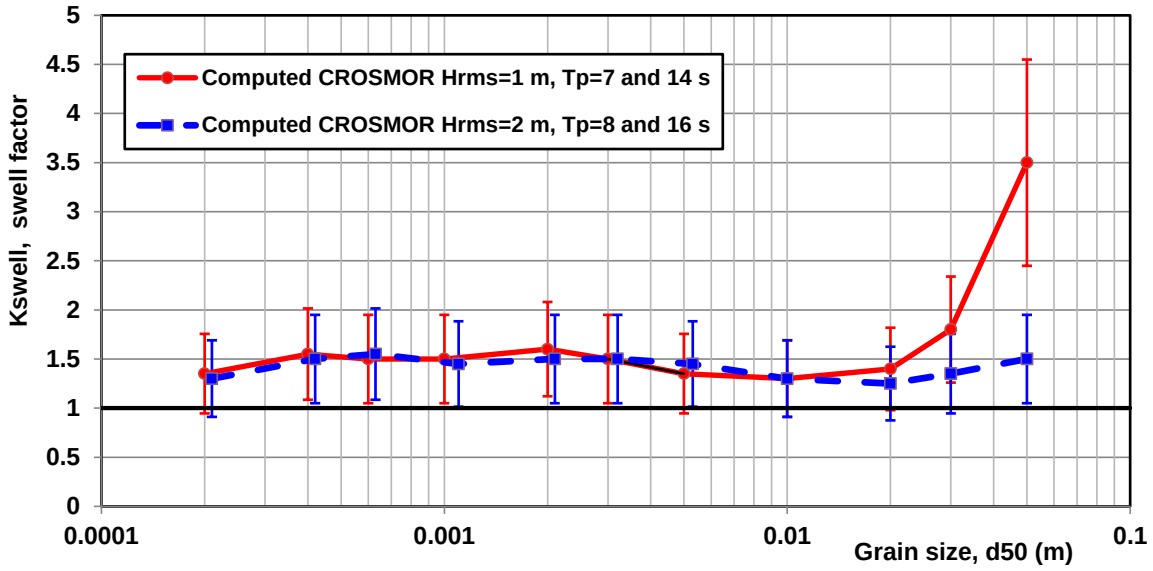

Figure 7 *Effect of wave type (regular or irregular waves) on longshore transport*

Figure 7 shows the swell effect as a function of grain size between 0.2 and 50 mm. The vertical variation expresses the effect of bed roughness variation and beach slope variation. The swell factor K_{swell} varies between 1.1 and 1.5 for grain sizes up to 50 mm in high swell of 2 m. In low swell of 1 m the swell effect is relatively large for very coarse grains of 30 and 50 mm. The lower waves of an irregular wave train (H_{rms}=1 m, T_p= 7 s) are much less able to transport the coarsest grains resulting in relatively low values of the longshore transport ($Q_{t,ww}$).

3.4.2 Grain size effect

The CROSMOR model has been used to study the effect of the grain size on the longshore transport. The sediment size (d_{50}) has been varied between 0.2 and 100 mm for one wave condition, being an offshore wave incidence angle of 30° and offshore wave height of 3 m (θ=30°, $H_{s,o}$= 3 m, T_p= 8 s; no tide). The cross-shore bed profile consisted of a plane bed without breaker bars.

The beach slope was 1 to 30 and 1 to 60 between -1 m and +3 m for grain sizes smaller than 2 mm and 1 to 10 and 1 to 20 for larger grain sizes. The surf zone slope was 1 to 60 between -6 m and -1 m. The sea bed slope between -6 and -20 m was 1 to 200.

The CROSMOR-model computes both the bed load and suspended load transport. The total longshore transport is the sum of both values. Suspended load transport is dominant for grain sizes smaller than about 1 mm for given conditions; bed load transport is dominant for grain sizes larger than 3 mm. The effect of the grain size on the longshore transport rate is given in terms of a grain size factor (K_{grain}) as a function of the median grain size (d_{50}), see **Figure 8**. The K_{grain}-values have been computed as $K_{grain}=Q_t/Q_{t,ref}$ with Q_t=computed total longshore total transport rate (kg/s) and $Q_{t,ref}$= computed total longshore transport rate (kg/s) for $d_{50,ref}$= 0.0002 m (0.2 mm). The vertical variation range of the values of Figure 8 expresses the effect of bed roughness variation in the range of 0.02 to 0.05 m and the beach slope variation. The present model results should be seen as exploring results, as the bed profiles do not represent equilibrium conditions.

The results based on the CROSMOR-model show that the grain size effect can be represented by a trend line expressing that the longshore transport rate is proportional to $(d_{50,ref}/d_{50})^{0.6}$, see **Figure 8**. The computed longshore transport rate for d_{50}= 2 mm is a factor $10^{0.6}$ (about 4) smaller than that for d_{50}=0.2 mm. Thus, $K_{grain}= (d_{50,ref}/d_{50})^{0.6}$

and longshore transport is proportional to $(1/d_{50})^{0.6}$. This relationship ($LT \approx (1/d_{50})^{0.6}$) seems to be valid for grain sizes up to 30 mm.
This strong effect of grain size is mainly caused by the strong decrease of the suspended load transport for increasing grain sizes. The bed load transport for grain sizes between 0.2 and 20 mm remains fairly constant (within factor 2), but the suspended load transport decreases strongly to almost zero for grains of about 20 mm. For grains larger than 20 mm the bed load transport decreases almost linearly with increasing grain size, see also **Figure 8**.
The grain size effect of the Kamphuis (1991) formula is given by: $Q_t \approx (d_{50,ref}/d_{50})^{0.25}$, see Equation (4a). The grain size effect of the Kamphuis (1991) formula is much smaller than that based on the CROSMOR-model, see Figure 8. This explains why the longshore transport formula of Kamphuis (1991) is not really valid for shingle (>10 mm). Mil-Homens et al. (2013) have recalibrated the Kamphuis formula and found that LT is proportional to $(1/d_{50})^{0.69}$, see **Figure 8**. The grain size effect of the modified Kamphuis formula (see Equation 4b) fits the CROSMOR-data quite well. Based on all this, it is concluded that the grain size effect of longshore transport is proportional to $(1/d_{50})$ to the power 0.6 or 0.7 over a large size range of 0.1 to 100 mm.

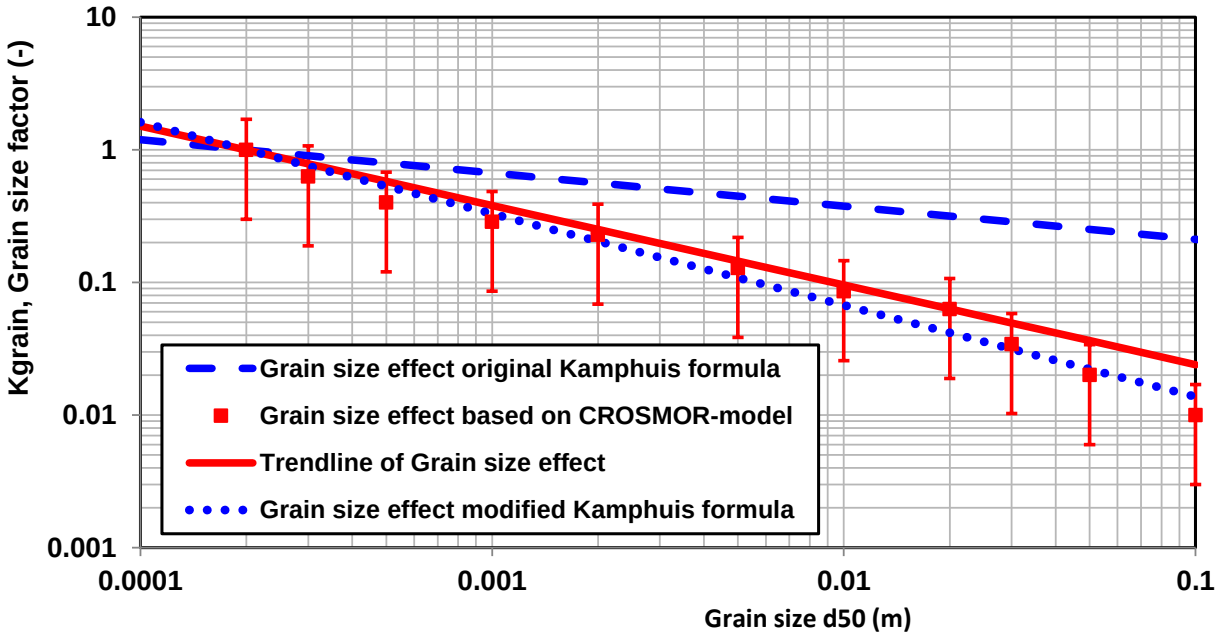

Figure 8 *Effect of particle size on longshore transport, offshore wave angle=30°, offshore wave height= 3 m, wave period= 8 s, at depth of 20 m*

3.4.3 Effect of profile shape

The CROSMOR model has been used to make a series of runs for various types of bed profiles to study the effect of beach/surf zone slopes. The smoothed profiles were taken from (see **Figure 9**):

- Egmond site (The Netherlands); profile with two major bars, the profile slope of the surf zone between the water line and the -8 m depth contour is approximately $\tan\beta = 0.01$, $d_{50} = 0.2$ mm;
- Noordwijk site (The Netherlands), relatively flat profile ($\tan\beta = 0.007$) with two bars, $d_{50} = 0.2$ mm;
- Duck site (Atlantic coast, USA); relatively steep profile ($\tan\beta = 0.015$) with two minor bars, $d_{50} = 0.2$ mm.

The computations for these three cases were carried out for conditions with a wave incidence angle of 30° and offshore wave heights of 3 m and peak wave period of 8 s. The particle diameter is 0.2 mm for all three cases.
Analysis of the results shows a substantial effect of the profile shape. A steeper profile yields a smaller surf zone but larger wave heights and larger longshore current velocities due to more intense wave breaking.
A relatively steep profile (Duck profile) leads to somewhat larger wave heights at the breaker line (defined at location where 5% of the waves are breaking) and somewhat larger longshore current velocities in the surf zone, compared with the values at the Egmond site. Consequently, the longshore sand transport rates are larger

($K_{slope}=Q_{t,Duck}/Q_{t,Egmond}=1.5$) than the values based on the Egmond profile. Similarly, a relatively flat profile (Noordwijk profile) leads to smaller wave heights at the breaker line and smaller longshore current velocities in the surf zone. As a result the longshore sand transport rates are significantly smaller ($K_{slope}=Q_{t,Noordwijk}/Q_{t,Egmond}= 0.7$). In addition, various plane bed profiles (no breaker bars) have been used with grain sizes in the range of 0.2 to 1 mm and surf zone slopes between -6 m and +3 m in the range between $\tan\beta=0.005$ and 0.1. The offshore bed slope is 1 to 200 between -20 m and -6 m. The offshore wave angle is 30°, the significant offshore wave height = 2.5 m, the peak wave period is 8 s. All results are plotted in **Figure 10**. The vertical variation range expresses the effect of bed roughness variation in the range of 0.02 to 0.05 m. For slopes ($\tan\beta$) in the range of 0.01 to 0.05 the longshore transport increases due to the dominant effect of larger wave heights and larger longshore current velocities. The bed slope effect is computed as: $K_{slope}=Q_t/Q_{t,ref}$ with $Q_{t,ref}$ = longshore transport for reference slope of 0.01. For bed slopes in the range of 0.05 to 0.1 the longshore transport based on the CROSMOR-model decreases somewhat due to the dominant effect of a relatively small surf zone. Based on all results, the profile shape effect can be crudely represented by $(\tan\beta)^{0.4}$, see trendline in Figure 10. The slope effect of the original Kamphuis 1991 formula (Equation 4a) is also shown in Figure 10. The slope effect of Kamphuis 1991 is much too strong for relatively steep slopes (between 0.05 and 0.1). The slope effect of the modified Kamphuis formula (Equation 4b) is also shown and is even stronger than that of the original formula.

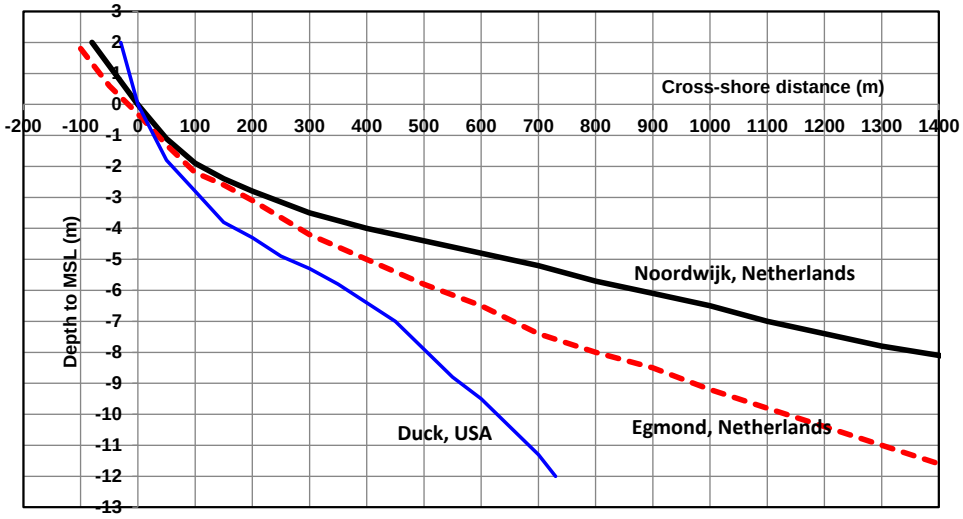

Figure 9 *Cross-shore profiles at Egmond (The Netherlands), Noordwijk (The Netherlands) and Duck (USA)*

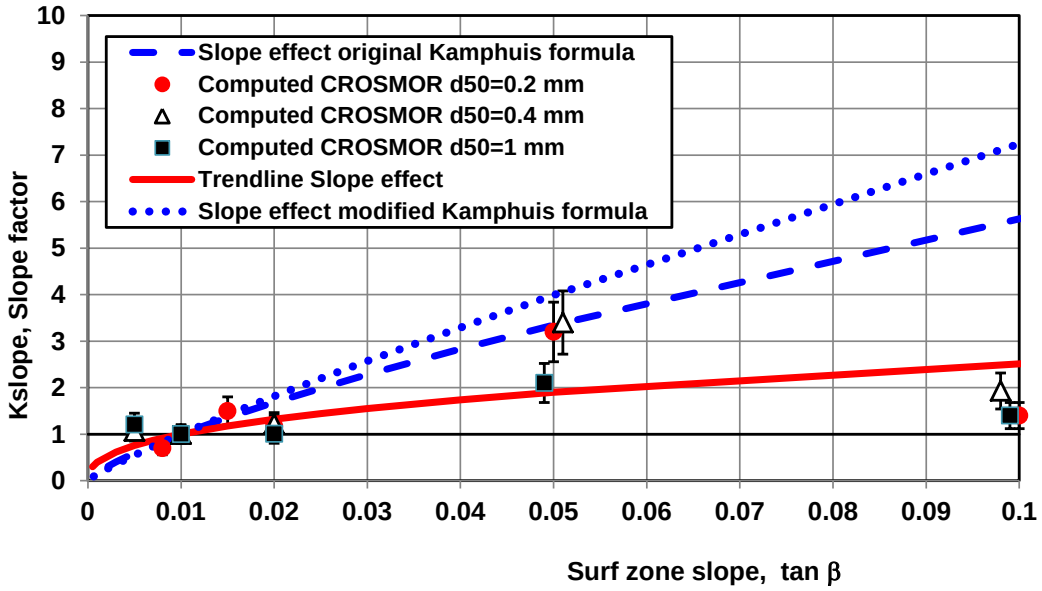

Figure 10. *Effect of beach/surf zone slope on longshore transport*

4 Simple general equation for longshore transport of sand, gravel and shingle

4.1 Derivation of general equation for longshore transport

Based on the CROSMOR-results (LT proportional to $d_{50}^{-0.6}$ and $\tan\beta^{0.4}$), it is assumed that the longshore transport rate ($Q_{t,mass}$ in kg/s) can be represented by the following (dimensionally correct) expression:

$$Q_{t,mass} = \alpha\, M \qquad (5)$$

with: M = mobility parameter (in kg/s) = $\rho_s\, g^{0.5}\, (\tan\beta)^{0.4}\, (d_{50})^{-0.6}\, (H_{s,br})^{3.1}\, \sin(2\theta_{br})$, Q_t= total longshore sediment transport (in kg/s), ρ_s =sediment density (kg/m^3), d_{50}= median grain size (m), $H_{s,br}$= significant wave height at breakerline (m), θ_{br} = wave angle at breakerline (degrees), α=calibration coefficient = 0.00018.
The power of the wave height was found to be about 3 (see **Figure 1**), but now it is raised to 3.1 for dimensional reasons.The calibration coefficient was found by fitting of Equation (5) to the sand and shingle data of Tables 1 and 2. The fit of the longshore transport rate as function of the mobility parameter M is given in **Figure 11**. About 80% of the 22 data points are within a factor 2 of the trend line.
Thus:

$$Q_{t,mass} = 0.00018\, \rho_s\, g^{0.5}\, (\tan\beta)^{0.4}\, (d_{50})^{-0.6}\, (H_{s,br})^{3.1}\, \sin(2\theta_{br}) \qquad (6)$$

Q_t= total longshore sediment transport (in kg/s), ρ_s =sediment density (kg/m^3), d_{50}= median grain size (m), $H_{s,br}$= significant wave height at breakerline (m), θ_{br} = wave angle at breakerline, g= acceleration of gravity (m/s^2), $\tan\beta$= slope of beach/surf zone.
Equation (6) includes the effects of grain size (trendline of Figure 8) and beach/surf zone slope (trendline of Figure 10) based on the CROSMOR results for grain sizes in the range of 0.1 to 100 mm and slopes in the range of 0.01 to 0.1. The slope effect is based on computations with grain sizes in the range of 0.2 to 1 mm. The inner surf zone slope should be used for sand beaches (< 2 mm) and the beach slope for shingle (2 to 50 mm). Equation (6) may underpredict gravel/shingle longshore transport for very low waves (< 0.5 m).

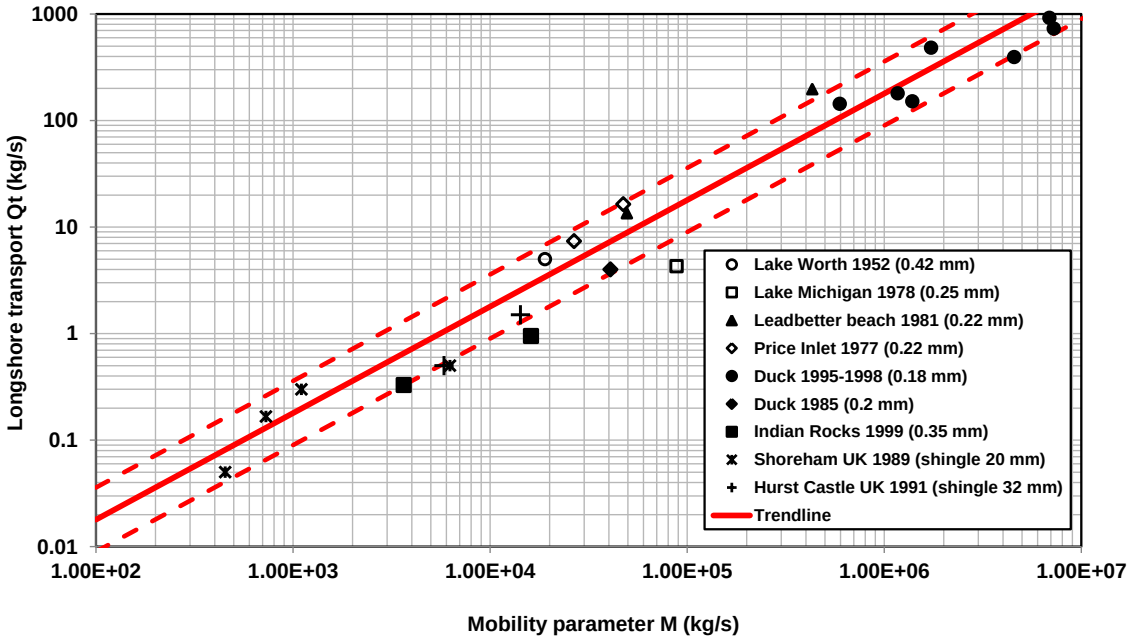

Figure 11 *Longshore transport of sand, gravel and shingle as function of mobility parameter*

Equation(6) does not account for the effect of the wave period on the longshore transport rate. However, low-period swell waves in the range of 1 to 2 m produce significantly larger transport rates (factor 1.5, see **Figure 7**) compared to wind waves of the same height (H_{rms}=H). This effect can to some extent be taken into account by using a correction factor to the longshore transport rate, if the percentage of swell waves (in terms of wave height) of the total wave height record is known. Herein, it is proposed to use a swell factor, as follows:

$$K_{swell}=1.5(p_{swell}/100) + 1\ (1-p_{swell}/100) = 0.015p_{swell} + (1-0.01p_{swell}) \quad (7)$$

with: p_{swell}= percentage of low-period swell wave heights of the total wave height record (about 10% to 20% for sea coasts and 20% to 30% for ocean coasts). Some values are: K_{swell}=1.05 for p_{swell}=10%; K_{swell}=1.1 for p_{swell}=20% and K_{swell}=1.5 for p_{swell}=100%. If swell is absent (or unknown), then K_{swell}= 1. Using this approach, the longshore transport rate increases slightly with increasing percentage of swell. The swell factor is based on computations with grain sizes in the range of 0.2 to 50 mm.
Based on this, Equation (6) reads, as:

$$Q_{t,mass}= 0.00018\ K_{swell}\ \rho_s\ g^{0.5}\ (\tan\beta)^{0.4}\ (d_{50})^{-0.6}\ (H_{s,br})^{3.1}\ \sin(2\theta_{br}) \quad (8)$$

Equation (8) can also be expressed, as:

$$Q_{t,mass}= 0.0006\ K_{swell}\ \rho_s\ (\tan\beta)^{0.4}\ (d_{50})^{-0.6}\ (H_{s,br})^{2.6}\ V_{wave} \quad (9)$$

$$V_{wave}= 0.3\ (gH_{s,br})^{0.5}\ \sin(2\theta_{br}) \quad (10)$$

with: V_{wave}= wave-induced longshore current velocity (m/s) averaged over the cross-section of the surf zone based on the work of Bagnold (1963) and Komar (1979).

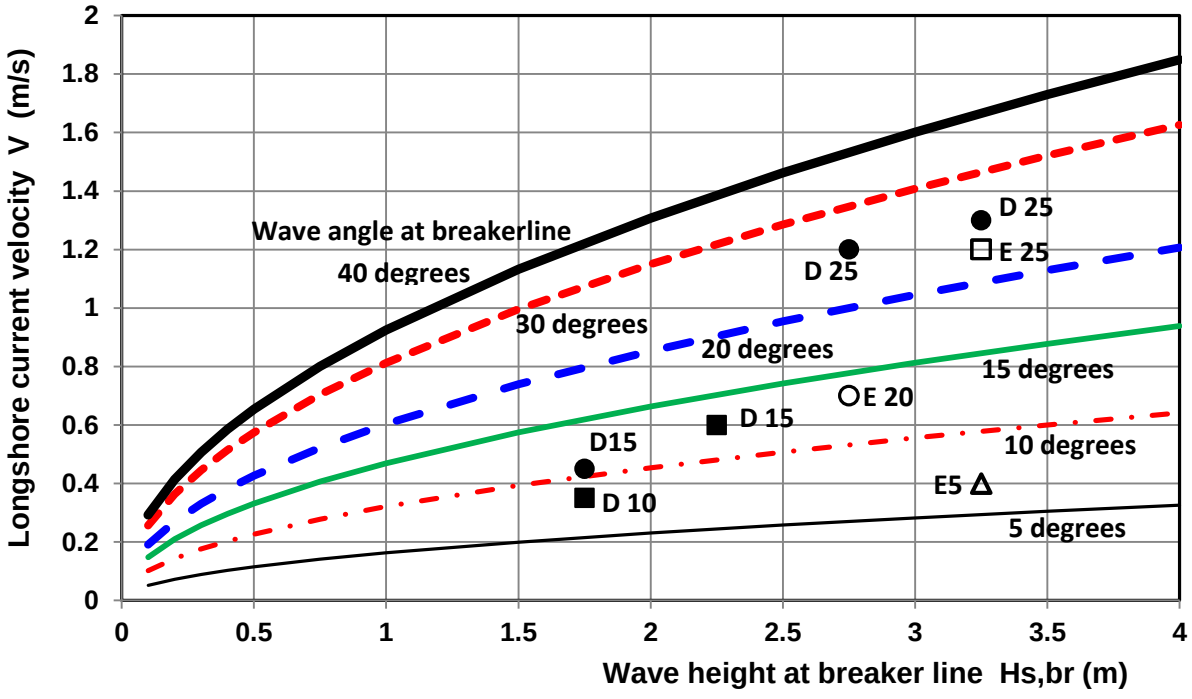

Figure 12 *Longshore current as function of wave height and wave angle at the breakerline (E25= measured velocity at Egmond site with wave angle at breakerline=25 degrees; D15= Duck site)*

The coefficient 0.3 of Equation (10) was determined by calibration using the CROSMOR-model for various schematized cases. Equation (10) is shown in **Figure 12** for wave incidence angles at the breakerline (θ_{br}) between 5° and 40°. The computed velocities vary between 0.1 and 2 m/s. To show that these values are realistic, some measured longshore velocities at the Egmond site (Van Rijn et al., 2002) and at the Duck site (Gallagher et al., 1998) are also plotted in **Figure 12**. The differences between measured and computed values are of the order of 20% to 30%.
Equation (10) is linear in velocity. Additional velocities in the surf zone due to tide and wind can be simply taken into account by schematizing the tidal period in two blocks, as follows:

$$V_{total} = V_{wave} + 0.01p_1 V_1 + 0.01p_2 V_2 \quad (11)$$

with V_1= representative velocity in positive longshore direction due to wind and tide; V_2= representative tidal velocity in negative longshore direction due to wind and tide; p_1= percentage of time with positive flow (about 50%), p_2= percentage of time with negative flow (about 50%). The peak longshore velocities in the surf zone due to wind and tide are approximately in the range of 0.1 m/s for micro-tidal to 0.5 m/s for macro-tidal conditions. Generally, there is a slight asymmetry in the wind-generated velocities in the main wave (wind) direction. Using this approach, a slight asymmetry in the velocities due to wind and tide (V_1 larger than V_2 or reversed) can be taken into account. The effect is zero in fully symmetric tidal flow (p_1=50%, p_2=50%, V_1=-V_2).

4.2 Wave refraction for uniform coasts

Equation (8 or 9) depends on the basic wave parameters at the breaker line. If only the offshore wave parameters are known, the values at the breakerline can be determined from refraction theory (Van Rijn, 1990/2011).
Assuming a straight uniform coast with parallel depth contours, the water depth at the breakerline (location where 5% of the waves are breaking) can be estimated from:

$$h_{br} = [(H_{s,o}^2 c_o \cos\theta_o)/(\alpha \gamma^2 g^{0.5})]^{0.4} \quad (12)$$

The wave incidence angle at the breakerline (θ_{br}) can be determined from:

$$\sin\theta_{br} = (c_{br}/c_o) \sin\theta_o \quad (13)$$

with: $H_{s,o}$ = significant wave height at deep water; h_{br} = water depth at breakerline; c_o, c_{br} = wave propagation speed at deep water and at breakerline; θ_o, θ_{br} = wave incidence angle (to shore normal) at deep water and at breakerline;
$\gamma = H_{s,br}/h_{br}$= breaking coefficient based on 5% breaking= 0.6 to 0.8; α = 1.8= calibration coefficient based on Egmond data; L_o = wave length in deep water (h_o), $c_o = L_o/T_p$, T_p= peak wave period.

4.3 Example computation

The following offshore values are given: h_o=20 m (water depth deep water), $H_{s,o}$= 3 m, T_p= 10 s, θ_o= 30 degrees; no swell (K_{swell}=1). The wave breaking coefficient is: γ=0.6. The sediment size is d_{50}=0.0003 m. The surf zone slope is $\tan\beta$= 0.02.
The wind- and tide induced velocities in the surf zone are: v_1=+0.2 m/s during p_1=50% of the time and V_2=-0.1 m/s during p_2=50% of the time.
This results in: L_o=121.2 m (wave length in water depth of 20 m), $c_o = L_o/T_p$= 12.1 m/s, h_{br}=4.65 m (water depth at breakerline), H_{br}=2,79 m, θ_{br}= 15,7 degrees, $\sin(2\theta_{br})$= 0.52, V_{wave}=0.815 m/s, V_{total}=0.864 m/s

The computed longshore transport rate is Q_t=630 kg/s (including tide-induced velocity) and Q_t=507 kg/s (excluding tide-induced velocities).

5 Verification of simplified longshore transport formula

Various field and laboratory cases have been used to verify Equation (8 or 9). Both short-term and long-term data of longshore transport have been used. The short-term data refer to field sites where the longshore transport rate was measured during short events (within a few hours) with constant wave conditions. The long-term data refer to field sites where the longshore transport rate was derived from budget studies and accretion against structures (harbour breakwaters). Two long-term sand cases (East African Ocean coast and Dutch North Sea coast) and one long-term shingle case (Shoreham coast, UK) with known net annual transport volumes have been selected for verification of the new expression. The annual prediction of longshore transport based on the mean annual wave climate is a rigorous test for the new expression, because the annual wave climate includes a wide range of conditions (wave height and wave angle at the breakerline).
Finally, the new equation for longshore transport has been compared to the modified Kamphuis formula (Mil-Homens et al., 2013). Mil-Homens et al. have found that modified Kamphuis formula produces the best score with about 56% within a factor of 2 of measured values for a large data set of about 250 data points (mostly sand beaches).

5.1 Short term field and laboratory data of coarse-grained beaches

Various reliable data sets (13) of coarse-grained beaches in field and laboratory conditions have been used to test Equation (8), see **Table 3**.
The longshore transport rate of coarse materials (in the range of 0.68 to 2.25 mm, see **Table 3**) was measured by Wang et al. (1998) using streamer traps (typical trap duration of 5 minutes) at several locations along the southeast coast of the US and the Gulf Coast of Florida. The transport rate was also measured concurrently by traps and by short-term impoundment (plywood structure normal to the shore) at Indian Rocks, west-central Florida. Wang et al. state that for their measurements the transport rates based on streamer traps are systematically smaller (factor 2 to 3) than that based on the impoundment method. Therefore, the measured values based on the streamer traps have herein been multiplied with 2.5. Furthermore, the measured values were converted from m^3/year to kg/s using a bulk density of 1600 kg/m^3. The basic data are given in **Table 3**. Most experiments were executed during relatively low wave conditions. The grain sizes were determined from various bed samples in the surf zone at the trap location. The measured H_{rms} was herein converted to significant wave height using $H_{s,br}$=1.41 $H_{rms,br}$.

Moore and Cole (1960) have studied the longshore transport of sand (d_{50}=1 mm) along a spit at Cape Thompson, northwestern Alaska (USA). They measured the growth of a newly formed spit across a temporary outlet of a lagoon. After a period of 3 hours, a total of 450 m^3 (or 0.0414 m^3/s $\cong$ 66 kg/s) of coarse materials had moved onto the spit. During this period the wave height was about 1.68 m, the wave period was 5.5 s. the wave angle at breakerline was 25 degrees. The beach slope was about $\tan\beta \cong 0.1$.

Burcharth and Frigaard (1988) have measured longshore transport rates of coarse materials (d_{50}=19 mm) along a reshaping breakwater in a laboratory basin. The initial plane slopes of 1 to 1.5 were reshaped into s-type profiles with a slope of 1 to 5 due to wave attack. The longshore transport rate was determined from video recordings of coloured materials placed in the profile. The data of experiments with the same wave height have been averaged herein. The spread of the results due to variation of the wave period and wave spectrum is less than 20%.

All but one computed transport rates are within a factor of 2 of the measured values, see **Table 3** and **Figure 13**. Only, for very low waves at Indian Rocks, the computed longshore transport rate is a factor of 3 too small. This is understandable as the transport in the uprush zone above the waterline is neglected in the CROSMOR-model results, which form the basis of the new formula for longshore transport. Amazingly, the new longshore transport formula yields rather good results for laboratory experiments with small irregular waves and shingle type sediment under a very steep slope of 1 to 1.5. This steep slope was modified into a new s-type profile with longshore transport over a much wider zone than the swash zone only (Burcharth and Frigaard, 1988).

Field and laboratory data	d_{50} (mm)	tanβ (-)	$H_{s,br}$ (m)	θ_{br} (°)	T_p (s)	Measured $Q_{t,mass}$ (kg/s)	Predicted $Q_{t,mass}$ (kg/s)
Onslow beach,NC, USA (Wang, 1998)	2.25	0.094	0.85	12	6.0	5.3	5.5
Canaveral beach, FL, USA (Wang, 1998)	0.9	0.115	0.65	9	3.5	2.4	3.4
Melbourne beach, FL, USA (Wang, 1998)	1.5	0.158	0.7	2.5	3.5	0.75	1.02
Lido Key beach, FL, USA (Wang, 1998)	0.68	0.105	0.53	14	3.7	4.9	3.2
Redington beach, FL, USA (Wang, 1998)	0.85	0.125	0.5	8.4	4.5	1.9	1.5
Redington beach, FL, USA (Wang, 1998)	0.9	0.026	0.45	19.2	4.5	1.05	1.21
Indian Rocks, FL, USA (Wang, 1998)	1.38	0.191	0.27	10	2.8	0.35	0.21
Indian Rocks, FL, USA (Wang, 1998)	1.29	0.152	0.2	8.2	3.8	0.25	0.073
Cape Thompson (Moore and Cole 1960)	1.0	0.091	1.66	25	5.5	67	133
Lab. Exp. Ir. Waves G-H; Burcharth 1988	19	0.2	0.13	15-30	1.8-2.5	0.005	0.01
Lab. Exp. Ir. Waves C-D; Burcharth 1988	19	0.2	0.15	15-30	1.8-2.5	0.012	0.015
Lab. Exp. Ir. Waves L; Burcharth 1988	19	0.2	0.175	15-30	2.5	0.021	0.024
Lab. Exp. Ir. Waves E; Burcharth 1988	19	0.2	0.2	15-30	2.8	0.033	0.037

d_{50} = particle size; tanβ= beach/surf zone slope; $H_{s,br}$= significant wave height at breakerline;

θ_{br} = wave angle to shore normal at breakerline; T_p = peak wave period,

Table 3 *Longshore transport data of coarse-grained field sites and laboratory experiments*

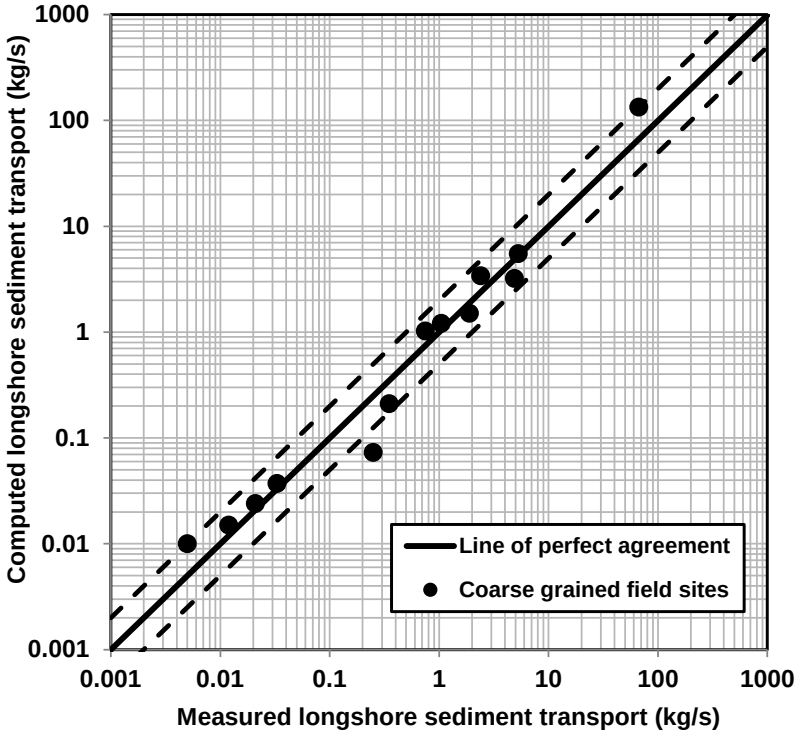

Figure 13 *Comparison of measured and computed longshore transport; coarse-grained beaches (0.68-19 mm)*

5.2 Long-term sand case; Richards Bay along Ocean coast of East Africa, South Africa

Richards Bay harbour is situated on the East African coast. The approach to the harbour is protected by two breakwaters. The local coastal topography north of the breakwaters is characterised by a relatively straight coastline with a narrow beach. The beach borders a relatively flat inland coastal plain at about 30 to 40 m above mean sea level. The local coast north of the port is a soft cliff type coast covered with bushes. The height of the cliffs varies in the range of 5 to 15 m. The beach is relatively narrow (about 50 m) and consists of fine to medium, reddish brown sand (grain sizes are in the range of 0.2 to 0.3 mm). Based on detailed studies, Swart (1981) concluded that the net longshore transport at Richards Bay is about 0.8 millions m^3/year towards the north-east. His results were confirmed by Laubscher et al. (1991). The high net transport values point to a very dynamic coast with large quantities of sand moving along the coast in both directions. The net longshore transport is directed north-eastward, which is in agreement with the accretion zone south of the southern breakwater at the entrance of Richards Bay and the erosion zone north of the northern breakwater. Based on the measured results of Schoonees (2000) for a sand trap south of the port of Durban, the net northgoing sand transport along the east coast of South-Africa between Durban and Richards Bay is estimated to be about 0.5 to 0.8 million m^3 per year. The sand trap values south of the port of Durban are in the range of 0.42 to 0.62 millions m^3 per year. The sand trap is dredged every year and the dredged volume is pumped onto the northern beach. A sand trap is also present at the beach south of the port entrance to Richards Bay from which sand is dredged and pumped onto the northern beach. Herein, it is assumed that the net longshore transport north of Richards Bay harbour is approximately 650.000 m^3/year (±150.000 m^3/year).

The tide is semi-diurnal at Richards Bay. The average neap tidal range is 0.52 m while the average spring tidal range is 1.8 m. The mean tidal range is about 1.15 m. The tidal flow through the port entrance is weak with values of about 0.1 to 0.15 m/s. Current velocity data measured over a 3 month-period in 1969 with a Kiel Hassee current meter positioned at 2 m above the local sea bed have been reported by Coppoolse and Schoonees (1991). The currents are weak with values in the range of 0.1 to 0.5 m/s. The dominant current directions are approximately parallel to the coastline. During major storm events the peak wind-driven current velocities are estimated to be in the range of 0.5 to 1 m/s.

The east coast of South Africa is exposed to waves from the Indian Ocean. These waves commonly have a long period swell component, with periods greater than about 10 s, and a shorter period due to locally generated waves. Most offshore significant wave heights are in the range of 1 to 3 m, with wave periods of 6 to 16 s and wave directions in the range of 60^o to 180^o. Corbella and Stretch (2012) have analysed wave data over the period of 1992 to 2009 offshore (depth of 22 m) of Richards Bay. Storm waves are generated off the coast by tropical cyclones, cold fronts and cut-off lows. Cold fronts generally move from west to east and exist closer to the coast. Tropical cyclones are very rare events. Only seven major storms affected the east coast since 1962. Generally, the tropical storm events produce north-easterly swells.

The wave data were analysed annually and seasonally in terms of the maximum wave height (H_{max}) of each record (about 30 min), the significant wave height (H_s), the peak wave period (T_p) and wave direction. The mean annual wave height is about 1.65 m. The mean annual wave period is about 11 s. The mean annual wave direction is rather constant (about 130^o). South-east is the most dominant wave direction, which is consistent with the observed direction of the net littoral drift (south-west to north-east). The largest waves occur in Autumn (March, April, May) and in winter (June, July, August). Summer is the calmest period (December, January and February). During summer the wave energy is spread almost evenly over the wave directions. The offshore wave data from the wave rose of the entire set (covering 18 years) have been summarized into **Table 4** with yearly-averaged wave data (5 wave height classes) for computation of the net longshore transport rate. Equations (12) and (13) have been used to compute the wave data at the breaker line. It has been assumed that 20% of the low waves are swell waves. The local shore normal (angle to the north) is set to 315^o. The local surf zone slope is set to $\tan\beta = 0.02$.

Wave direction to North (degrees)	Wave direction to shore normal (degrees)	Wave height $H_{s,o}$= 4 m T_p= 22 s	Wave height $H_{s,o}$= 3 m T_p= 18 s	Wave height $H_{s,o}$= 2.25 m T_p=15 s	Wave height $H_{s,o}$=1.75m T_p= 13 s	Wave height $H_{s,o}$=1.25 m T_p= 11 s	Wave height $H_{s,o}$=0.75 m T_p=10 s	Total (days)
75 (255)	-60	0 days per year	2 days per year	1	6	10	2	19
105 (285)	-30	0.3 days per year	3 days per year	8	30	41	6	88
135 (315)	0	0.8 days per year	5 days per year	11	29	46	8	99
165 (345)	30	0.9 days per year	8 days per year	17	44	69	11	119
All waves directions		2 days per year	16 days per year	37	109	166	27	357

Wave direction=direction to North from which the waves are coming (between brackets: the wave direction in which the waves are going); Shore normal (angle to north)=315; positive wave angle to shore normal yields transport to north-east (dominant transport direction)

Table 4 *Frequency of occurrence (number of days per year; total 365) based on offshore wave data of Corbella and Stretch (2012)*

Input parameters	Computed longshore transport rate to north (m^3/year)	Computed longshore transport rate to south (m^3/year)	Computed net longshore transport rate (m^3/year)	Measured net longshore transport rate (m^3/year)
Grain size d_{50}=0.0002 m Velocity difference $\Delta V=V_1-V_2$=0 m/s	1,350,000	780,000	570,000	650,000 (±150,000)
Grain size d_{50}=0.0003 m Velocity difference $\Delta V=V_1-V_2$=0 m/s	1,065,000	615,000	450,000	
Grain size d_{50}=0.0002 m Velocity difference $\Delta V=V_1-V_2$=0.05 m/s to north	1,460,000	750,000	710,000	
Grain size d_{50}=0.0002 m Velocity difference $\Delta V=V_1-V_2$=0.1 m/s to north	1,570,000	720,000	850,000	

Table 5 *Computed net longshore transport at Richards Bay, South Africa*

The net longshore transport rates have been computed using the excel programme LITTORAL.xls (free download www.leovanrijn-sediment.com) and are given in **Table 5**. The input parameters have been varied yielding a net longshore transport of sand in the range of 450,000 to 850,000 m^3/year (650,000±200,000 m^3/year). The velocities in the surf zone due to wind and tide have a significant effect on the results. Neglecting these additional velocities or assuming symmetric additional velocities ($\Delta V=V_1-V_2=0$), the net longshore transport is approximately 15% too small compared with the measured value (650,000 m^3/year) for 0.2 mm sand and about 30% too small for 0.3 mm sand.

The modified Kamphuis 2013 formula predicts a net longshore transport of 390,000 m^3/year. The original Kamphuis 1991 formula yields 550,000 m^3/year. Both values are too small. However, in this case the original Kamphuis formula performs much better than the modified formula.

5.3 Long-term sand case: Katwijk beach along Holland North Sea coast

The Holland North Sea coast consists of two long sections (North- and South-Holland; each with a length of about 50 km) separated by the long harbour breakwaters to the port of Amsterdam. Both coastal sections are at many places characterised by wide beaches and high dunes consisting of sand in the range of 0.2 to 0.25 mm. The semi-diurnal tidal range is about 2 m. The current velocity to the north in the surf zone due to wind and tide is in the range of about 0.2 to 0.3 m/s. The current velocity to the south is in the range of 0.1 to 0.2 m/s. Hence, the velocity difference is about $\Delta V=V_1-V_2=0.05$ to 0.15 m/s.

The mean annual wave climate used is based on long term wave measurements (height, period and angle) at various offshore wave stations in the period 1980 to 1990, see **Table 6**. The most important wave directions are between south-west and north-west. High wind waves generally are from the north-west direction due to the longer fetch. The dominant wave direction is, however, south-west resulting in a net longshore transport to the north-east. Waves larger than 0.75 m contributing to longshore transport are present during 108 days of the year. During the rest of the year the waves are either too small or from non-contributing directions.

The net annual longshore transport along the coast of South-Holland has been studied by Van Rijn (1997). Based on detailed analysis of long term (1980 to 1990) volume changes in the beach and surf zone including the regular nourishment volumes, the net annual longshore transport along the South-Holland coast was found to increase from about 150,000 m^3/year at the southern end near Hoek van Holland to about 500,000 m^3/year at the northern end near IJmuiden. Harbour breakwaters are situated at both ends. The beach site of Katwijk (about 23 km north of The Hague) is in the middle of the southern section far away from the long harbour breakwaters. The net annual transport at Katwijk is approximately 250,000±50,000 m^3/year. The local surf zone slope is $\tan\beta \cong 0.01$ to 0.02. The local shore normal is 125° to the north. Equations (12) and (13) have been used to compute the wave parameters at the breakerline. The wave breaking coefficient is set to 0.6. It has been assumed that 10% of the low waves are swell waves.

Significant wave height H_s (m)	**Peak wave period T_p (s)**	**Wave direction to shore normal θ (°)**	**Duration (days)**	**Significant wave height H_s (m)**	**Peak wave period T_p (s)**	**Wave direction To shore normal θ (°)**	**Duration (days)**
0.75	5	60	9.7	2.75	7	60	0.3
		-60	11.8			-60	2.0
		-30	9.1			-30	2.0
		30	8.9			30	1.1
1.25	6	60	6.2	3.25	8	60	0.1
		-60	10.4			-60	0.9
		-30	7.4			-30	1.1
		30	6.4			30	0.4
1.75	7	60	2.2	3.75	8	60	0.04
		-60	6.9			-60	0.4
		-30	5.3			-30	0.9
		30	3.5			30	0.1
2.25	7	60	0.4	4.25	9	-60	0.2
		-60	3.4			-30	0.4
		-30	3.4			30	0.07
		30	1.7	5.0	10	-60	0.1
						-30	0.4
						30	0.1
Total			97 days				11 days

Negative wave angle yields transport to north-east (dominant longshore transport direction)

Table 6 *Offshore (depth of 30 m) wave climate coast of South Holland*

Input parameters	Computed longshore transport rate to north (m^3/year)	Computed longshore transport rate to south (m^3/year)	Computed net longshore transport rate (m^3/year)	Measured net longshore transport rate (m^3/year)
Grain size d_{50}=0.0002 m Surf zone slope tanβ=0.01 Velocity difference $\Delta V=V_1-V_2$=0 m/s	480,000	225,000	255,000	250,000 (±50,000)
Grain size d_{50}=0.0002 m Surf zone slope tanβ=0.02 Velocity difference $\Delta V=V_1-V_2$=0 m/s	640,000	290,000	340,000	
Grain size d_{50}=0.00025 m Surf zone slope tanβ=0.01 Velocity difference $\Delta V=V_1-V_2$=0 m/s	420,000	195,000	225,000	
Grain size d_{50}=0.0002 m Surf zone slope tanβ=0.01 Velocity difference $\Delta V=V_1-V_2$=0.05 m/s to north	500,000	215,000	285,000	
Grain size d_{50}=0.0002 m Surf zone slope tanβ=0.01 Velocity difference $\Delta V=V_1-V_2$=0.1 m/s to north	515,000	200,000	315,000	

Table 7 *Computed net longshore transport at Katwijk, The Netherlands*

The computed net longshore transport rates using the excel programme LITTORAL.xls are given in **Table 7**. The input parameters have been varied yielding a net longshore transport of sand in the range of 225,000 to 340,000 m^3/year (280,000±60,000 m^3/year). The velocities in the surf zone due to wind and tide have a significant effect on the results. Neglecting these additional velocities or asssuming symmetric additional velocities ($\Delta V=V_1-V_2$=0), the net longshore transport is approximately equal to the measured value (250,000 m^3/year) for 0.2 mm sand and about 10% too small for 0.25 mm sand.

The modified Kamphuis 2013 formula predicts a net longshore transport of 100,000 m^3/year. The original Kamphuis 1991 formula yields 115,000 m^3/year. Both values are much too small (factor 2.5) compared to the measured value of 250,000 m^3/year.

5.4 Long-term shingle case: Shoreham beach at south coast along English Channel (UK)

The long-term (annual) field data of the Shoreham site in the UK (Van Wellen et al., 2000) have been used to check the predicting ability of the new expression for longshore transport of shingle. The Shoreham site along the English Channel is in a natural state over about 2 km. The prevailing wave direction is from the south-west resulting in net longshore transport to the east. To the east, the beach is confined by a long harbour breakwater. The toe of the shingle beach exceeds only halfway along the breakwater and therefore it can be assumed that no longshore transport of shingle occurs past the breakwater. The annual accumulation against the breakwater was found to be about 15,000 m^3/year with an inaccuracy range of ±50% (Van Wellen et al., 2000). The Shoreham harbour authorities have bypassed shingle eastward around the breakwaters at a rate of 8,500 m^3/year in the period 1992 to 2000 (Vaughan, 2001). The mean annual wave climate at the breakerline is given in tabulated form by Van Wellen et al. (2000), see also **Table 8**. It is noted that the wave data are not based on direct offshore wave measurements but are hindcasted from a four-year record of wind measurements in the period 1980 to 1984. The offshore wave data were transformed to values at the breakerline using wave refraction and shoaling theory. Using this approach based on wind measurements, the contribution of swell waves coming from the Atlantic Ocean is neglected.

The current velocities in the surf zone are estimated to be in the range of 0.1 to 0.3 m/s. The current velocities in deep water of the English Channel are as large as 2 m/s (www.scopac.org.uk). The d_{50} of shingle is about 0.02 m. The beach slope is 1 to 8.8 or $\tan\beta$=0.114. The porosity of the shingle material is assumed to be p=0.45.

Significant wave height Hs (m)	Wave period T (s)	Wave direction to shore normal θ (°)	Duration (days)	Significant wave height H_s (m)	Wave period T (s)	Wave direction to shore normal θ (°)	Duration (days)
0.14	3.4	-10	9.9	2.27	5.7	-5	2.0
0.37	3.8	-15	7.1	2.68	6.1	-6	0.5
0.6	4.3	-17	0.9	3.09	6.6	-7	0.1
0.86	4.8	-18	0.1	0.25	3.4	4	13.2
0.2	3.4	-10	11.9	0.65	3.8	6	6.7
0.54	3.8	-14	8.7	1.05	4.3	7	7.4
0.88	4.3	-16	3.0	1.43	4.8	6	7.7
1.21	4.8	-17	0.9	1.79	5.2	6	9.2
1.55	5.2	-18	1.5	2.12	5.7	5	5.2
1.9	5.7	-19	1.5	2.44	6.1	5	3.0
0.25	3.4	-7	6.8	2.77	6.6	4	1.1
0.67	3.8	-10	3.4	3.17	7.1	4	0.05
1.09	4.3	-12	3.4	0.19	3.4	7	13.2
1.48	4.8	-13	0.9	0.49	3.8	10	19.9
1.87	5.2	-14	0.4	0.8	4.3	11	24.1
2.24	5.7	-14	1.1	1.11	4.8	11	12.7
2.65	6.1	-15	1.1	1.41	5.2	11	6.6
0.27	3.4	-1	7.6	1.71	5.7	10	3.7
0.71	3.8	-2	3.5	1.98	6.1	10	1.0
1.15	4.3	-2	3.9	2.29	6.6	10	0.05
1.50	4.8	-3	2.9	0.13	3.4	7	21.4
1.88	5.2	-4	2.8	0.33	3.8	10	17.7
				0.54	4.3	11	4.7
				0.76	4.8	11	2.0
				0.96	5.2	11	0.2
Total			83				183 days

Positive wave angle yields transport to the east (dominant longshore transport direction)

Table 8 *Wave climate at breakerline of Shoreham beach (UK)*

Input parameters	Computed longshore transport rate to east (m^3/year)	Computed longshore transport rate to west (m^3/year)	Computed net longshore transport rate (m^3/year)	Measured net longshore transport rate (m^3/year)
Grain size d_{50}=0.02 m Velocity difference $\Delta V=V_1-V_2$=0 m/s	28,000	19,000	9,000	15,000 (±7,500)
Grain size d_{50}=0.015 m Velocity difference $\Delta V=V_1-V_2$=0 m/s	33,000	22,000	11,000	
Grain size d_{50}=0.030 m Velocity difference $\Delta V=V_1-V_2$=0 m/s	22,000	15,000	7,000	
Grain size d_{50}=0.02 m Velocity difference $\Delta V=V_1-V_2$=0.05 m/s to east	31,000	18,000	13,000	
Grain size d_{50}=0.02 m	33,000	17,000	16,000	

Velocity difference $\Delta V=V_1-V_2$=0.1 m/s to east				

Table 9 *Computed net longshore transport at Shoreham, UK*

The computed net longshore transport rates using the excel programme LITTORAL.xls are given in **Table 9**. The input parameters have been varied yielding a net longshore transport of shingle in the range of 7,000 to 16,000 m^3/year (12,000±5,000 m^3/year). The velocities in the surf zone due to wind and tide (assumed to be asymmetric to the east) have a significant effect on the results. Neglecting these additional velocities or assuming symmetric additional velocities ($\Delta V=V_1-V_2=0$), the net longshore transport is approximately 40% too small compared with the measured value (15,000 m^3/year). The modified Kamphuis 2013 formula predicts a net shingle transport of 8,500 m^3/year. The original Kamphuis 1991 formula yields a large overprediction of 55,000 m^3/year, which shows that this latter formula is not really valid for shingle beaches.

A reason for the underprediction may be the absence of swell in the wave record, see **Table 8** . An offshore swell of 1 m during 4 weeks per year at angle of 10 degrees to the shore normal yields an additional longshore transport of shingle to the east of about 4,000 m^3/year (based on Equation (6)).

5.5 Comparison of Longshore transport formula of Van Rijn and modified Kamphuis

The new formula of Van Rijn for longshore transport (Equation 8) has been compared to the modified formula of Kamphuis (Equation 4b). This latter formula has been developed based on computer fitting using about 250 data points (Mil-Homens et al., 2013) with a score of 56% within a factor of 2 of the measured values. Figure 14 shows the computed longshore transport rates as a function of wave height at the breakerline and grain size. The input values are given in **Table 10**. The wave angle at the breakerline is 20 degrees. Four grain sizes have been used: 0.2, 0.4, 1 and 20 mm (sand to shingle). The beach slope increases with grain size.

Wave angle at breakerline θ_{br} (degrees)	**Significant wave height at breakerline $H_{s,br}$ (m)**	**Peak wave period T_p (s)**	**Grain size d_{50} (m)**	**Beach slope tanβ (-)**
20	0.5	5	0.0002	0.02
20	1.0	5.5	0.0004	0.03
20	1.5	6.0	0.001	0.05
20	2.0	6.5	0.02	0.1
20	2.5	7.0		
20	3.0	8.0		
20	3.5	9.0		
20	4.0	10.0		

Table 10 *Input values*

The longshore transport increases strongly with increasing wave height and decreases with increasing grain size. The longshore transport of shingle (20 mm) is a factor of 10 smaller than that of sand of 0.2 mm. The formula of Van Rijn yields values which are roughly a factor of 3 larger than that of the modified Kamphuis formula for sand and a factor of 2 for shingle. These differences are somewhat smaller for a wave angle of $\theta_{br}=10^o$.

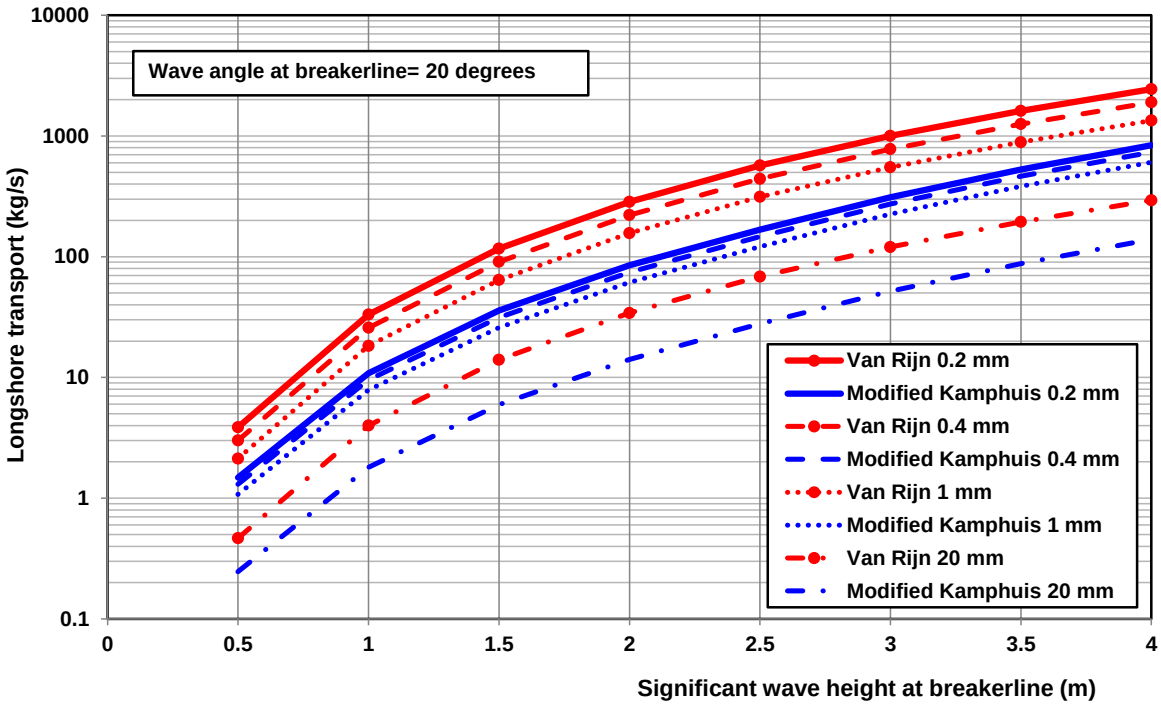

Figure 14 *Longshore transport as function of wave height at breakerline and grain size based on the formulas of Van Rijn and modified Kamphuis*

6 Conclusions

Longshore transport of sand, gravel and shingle has been studied using field and laboratory data over a wide range of conditions. The available field data cover a transport range between about 0.1 and 1000 kg/s. A detailed model (CROSMOR) for cross-shore and longshore sediment transport has been used to determine the effects of wave period, grain size, beach/surf zone slope and type of waves (wind waves or swell waves). The longshore transport was found to be proportional to wave height to the power 3.1 ($\approx H^{3.1}$), to grain size to the power -0.6 ($\approx d_{50}^{-0.6}$) and to beach slope to the power 0.4 ($\approx \tan\beta^{0.4}$). The longshore transport is significantly affected by the profile shape; a relatively steep profile (Duck profile) leads to somewhat larger wave heights at the breakerline and somewhat larger longshore current velocities and transport rates in the surf zone, compared to the values at the more gentle Egmond profile. Similarly, a relatively flat profile (Noordwijk profile) leads to smaller wave heights at the breakerline and smaller longshore current velocities and transport rates in the surf zone.The effect of slope on longshore transport is not yet fully certain. Data analysis performed by Mil-Homens et al. (2013) shows a power of almost 0.9. However, the slopes of coarse grained beaches of their data have not always been measured but often they have been derived from d_{50}-values assuming a Dean equilibrium profile (personal communication Mil-Homens). Furthermore, the data set of Mil Homens contains only few data of coarse grained beaches.

Regular swell waves yield much larger (factor 1.5) longshore transport rates than irregular wind waves of the same height. It is proposed to take this effect into account by a swell correction factor. Short-term and long-term field data of sand, gravel and shingle have been used for verification of the new longshore transport formula. In most cases the predicted longshore transport rates are within a factor of 2 of the measured values. The new formula also yields rather good results for longshore transport of coarse material along a breakwater in a laboratory basin.

The CERC and Kamphuis 1991 formulas have also been tested. The CERC formula yields results, which are slightly too large (factor 2) compared with measured values for storms but are much too large (factor 5) for low wave conditions. The original Kamphuis formula (1991) yields results, which are slightly too small (factor 1.5) for storm conditions but much too large (factor 3) for low wave conditions. These results are in agreement with the findings of Mil-Homens et al. (2013). The modified Kamphuis formula (2013) also overpredicts for low waves and

underpredicts for high waves, but less than the original formula. The modified Kamphuis formula did not perform well (significant underprediction) for both long-term sand cases (Richards Bay, South Africa and Katwijk, The Netherlands), which is somewhat strange as the formula performs quite well for the short-term data (Mil-Homens et al., 2013). As regards the long-term shingle case of Shoreham (UK), the modified Kamphuis formula performs well, but the prediction of the original formula is much too large (factor 3 to 4).

Overall, it can be concluded that a new and simple formula (Equation 8 or 9) for the total longshore transport consisting of bed load and suspended load is now available, which can be used for sand, gravel and shingle beaches. The formula is broadly valid for grain sizes between 0.1 and 100 mm. The key influencing parameters are: significant wave height and wave angle at the breakerline, the d_{50} and the slope of the beach material. The new formula is believed to underpredict for very low waves (<0.5 m) at gravel/shingle beaches due to poor representation of the longshore transport in the uprush zone above the mean waterline. The swash-type transport is neglected in the CROSMOR-model results, which form the basis of the new formula.

7 Acknowledgements

Richard Soulsby is gratefully acknowledged for his comments to improve the manuscript.

8 References

Bagnold, R.A., 1963. Mechanics of Marine Sedimentation, in: The Sea, Vol. 3, p. 507-528, edited by M.N. Hill, Interscience, NY

Burcharth, H.F. and Frigaard, P., 1988. On the 3D stability of reshaping breakwaters. 21st ICCE, Malaga, 2284-2298

Chadwick, A.J., 1989. Field measurements and numerical model verification of coastal shingle transport. Advances in Water Modelling and Measurement BHRA, 381-402

Coppoolse, R.C. and Schoonees., J.S., 1991. Maintenance dredging at Richards Bay; sensitivity analysis of predictive models and the location of an offshore dumpsite. CEDA Dredging Day, Amsterdam.

Corbella, S. and Stretch, D.D., 2012. The wave climate on the Kwazulu-Natal coast of South Africa. Journal of the South-African Institution of Civil Engineering, Vol. 54, No. 2, 45-54.

Damgaard, J.S. and Soulsby, R.L.,1997. Longshore bed-load transport, 25th ICCE, Orlando, USA, 3614-3627

Damgaard, J.S. and Soulsby, R.L., 2005. Bedload sediment transport in coastal waters. Coastal Engineering 52, 673-689

Dally, W.R. and Osiecki, D.A., 1994. The role of rollers in surf zone currents. Proc. 24th ICCE, Kobe, Japan

Davies, A.G. and Villaret, C., 1997. Oscillatory flow over rippled beds. In: J.N. Hunt (ed.), Gravity waves in water of finite depth: Chapter 6, 215-254. Advances in fluid mechanics, Computational Mechanics Publications

Davies, A.G. and Villaret, C., 1998. Wave-induced currents above rippled beds, 187-199. In: Physics of estuaries and coastal seas, edited by J. Dronkers and M. Scheffers, Balkema, Brookfield

Davies, A.G. and Villaret, C., 1999. Eulerian drift induced by progressive waves above rippled and very rough bed, 1465-1488. Journal of Geophysical Research, Vol. 104, No. C1

Gable, C.G., 1981. Report on data from NSTS experiments at Leadbetter Beach, Santa Barbara, California. University of California, Institute of Marine Resources, Rep. No. 80-5

Gallagher, E.L., Elgar, S. and Guza, R.T., 1998. Observations of sand bar evolution on a natural beach. Journal of Geophysical Research, Vol. 103, N0. C2, 3203-3215

Grasmeijer, B.T., 2002. Process-based cross-shore modelling of barred beaches. Doctoral Thesis. Department of Physical Geography, University of Utrecht, Utrecht, The Netherlands

Grasmeijer, B.T. and Van Rijn, L.C., 1998. Breaker bar formation and migration. Proc.26th ICCE, Copenhagen, Denmark

Houwman, K.T. and Ruessink, B.G., 1996. Sediment transport in the vicinity of the shoreface nourishment of Terschelling. Dep. of Physical Geography. University of Utrecht, The Netherlands

Isobe, M. and Horikawa, K., 1982. Study on water particle velocities of shoaling and breaking waves. Coastal Engineering in Japan, Vol. 25.

Kamphuis, J.W. 1991. Alongshore sediment transport rate. Journal of Waterway, Port, Coastal and Ocean Engineering, Vol. 117, 624-640

Kana, T.W. et al., 1977. Suspended sediment transport at Price Inlet. Coastal Sediments, 1069-1088

Kana, T.W and Ward, L.G., 1980. Nearshore suspended sediment load during storm and post-storm conditions. 17th ICCE, Sydney, Australia, 1158-1173

Komar, P.D. ,1979. Beach slope dependence of longshore currents. Journal of Waterway, Port, Coastal and Ocean Division, ASCE, Vol. 105, WW 4

Kraus, N.C. and Dean, J.L., 1987. Longshore sediment transport rate distributions measured by trap. Coastal Sediments, New Orleans, USA, 881-896

Laubscher, W.I., Coppoolse, R.C., Schoonees, J.S. and Swart, D.H., 1991. A calibrated longshore transport model for Richards Bay. Coastal Sediments, Seattle, Canada.

Lee, K.K., 1975. Longshore currents and sediment transport in West Shore of Lake Michigan. Water Resources Research, Vol. 11, No. 6, 1029-1032

Mil-Homens, J., Ranasinghe, R., Van Thiel de Vries, J.S.M. and Stive, M.J.F., 2013. Re-evaluation and improvement of three commonly used bulk longshore sediment transport formulas. Coastal Engineering 75, 29-39

Miller, H.C., 1999. Field measurements of longshore sediment transport during storms. Coastal Engineering, Vol. 36, 301-321

Moore, G.W. and Cole, J.Y., 1960. Coastal processes in the vicinity of Cape Thompson, Alaska. In: Geologic investigations in support Project Chariot in the vicinity of Cape Thompson, northwestern Alaska. U.S. Department of Interior, Geological Survey, USA

Nicholls, R.J. and Wright, P., 1991. Longshore transport of pebbles: experimental estimates of K-factor. Coastal Sediments, 1563-1577

Ruessink, B.G., Ramaekers, G. and Van Rijn, L.C., 2012. On the parameterization of the free-stream non-linear wave orbital motion in nearshore morphodynamic models. Coastal Engineering 65, 56-63

Schoonees, J.S., 2000. Annual variation in the net longshore sediment transport rate. Coastal Engineering 40, 141-160.

Schoonees, J.S. and Theron, A.K., 1993. Review of the field-data base for longshore sediment transport. Coastal Engineering, Vol. 19, 1-25

Schoonees, J.S. and Theron, A.K., 1996. Improvement of the most accurate longshore transport formula. 25th ICCE Orlando, USA

Shore Protection Manual, 1984. CERC, Waterways Experiment Station, Vicksburg, USA

Svendsen, I.A., 1984. Mass flux and undertow in the surf zone. Coastal Engineering, Vol. 8, 347-365

Swart, H., 1981. Effect of Richards Bay Harbour development on the adjacent coast. 25th Congress, PIANC, Edinburgh, Section II, Vol. 5, 899-917.

Tomasicchio, G.R., D'Alessandro, Barbaro, G. and Malara, G., 2013. General longshore transport model. Coastal Engineering 71, 28-36

Van Rijn, L.C., 1990, 2011. Principles of fluid flow and surface waves in rivers, estuaries and coastal seas. Aqua Publications, Nederland (www.aquapublications.nl)

Van Rijn, L.C., 1997. Sediment transport and budget of the central coastal zone of Holland. Coastal Engineering, Vol. 32, 61-90

Van Rijn, L.C., 1993, 2006. Principles of sediment transport in rivers, estuaries and coastal seas. Aqua Publications, Netherlands (www.aquapublications.nl)

Van Rijn, L.C., 2002. Longshore transport. 28th ICCE, Cardiff, UK, 2439-2451

Van Rijn, L.C., 2006, 2012. Principles of sedimentation and erosion engineering in rivers, estuaries and coastal seas. Aqua Publications, The Netherlands (www.aquapublications.nl)

Van Rijn, L.C., 2007a. Unified view of sediment transport by currents and waves, I: Initiation of motion, bed roughness and bed-load transport. Journal of Hydraulic Engineering, ASCE, Vol. 133, No. 6, 649-667

Van Rijn, L.C., 2007b. Unified view of sediment transport by currents and waves, II: Suspended transport. Journal of Hydraulic Engineering, ASCE, Vol. 133, No. 6, 668-689

Van Rijn, L.C., 2007c. Unified view of sediment transport by currents and waves, III: Graded beds. Journal of Hydraulic Engineering, ASCE, Vol. 133, No. 7, 761-775

Van Rijn, L.C., 2007d. Unified view of sediment transport by currents and waves, IV: Application of morphodynamic model. Journal of Hydraulic Engineering, ASCE, Vol. 133, No. 7, 776-793

Van Rijn, L.C., 2009. Erosion of gravel/shingle beaches and barriers. Report EU-Project CONSCIENCE, Deltares, Delft, The Netherlands

Van Rijn, L.C. and Wijnberg, K.M., 1994. One-dimensional modelling of individual waves and wave-induced longshore currents in the surf zone. Report R 94-09, Dep. of Physical Geography, Univ. of Utrecht.

Van Rijn, L.C. and Wijnberg, K.M., 1996. One-dimensional modelling of individual waves and wave-induced longshore currents in the surf zone. Coastal Engineering, Vol. 28, 121-145

Van Rijn, L.C. and Sutherland, J.R., 2011. Erosion of gravel barriers and beaches. Coastal Sediments, Miami, USA

Van Rijn, L.C., Ruessink,B.G. and Mulder, J.P.M., 2002. COAST3D-Egmond; The behaviour of a straight sandy coast on the time scale of storms and seasons. Aqua Publications, Netherlands (www.aquapublications.nl)

Van Rijn, L.C., Walstra, D.J.R., Grasmeijer, B., Sutherland, J., Pan, S. and Sierra, J.P., 2003. The predictability of cross-shore bed evolution of sandy beaches at the time scale of storms and seasons using process-based models. Coastal Engineering, 47, 295-327

Van Rijn, L.C., Tonnon, P.K. and Walstra, D.J.R., 2011. Numerical modelling of erosion and accretion of plane sloping beaches at different scales. Coastal Engineering, Vol. 58, 637-655

Van Wellen, E., Chadwick, A.J. and Mason, T., 2000. A review and assessment of longshore sediment transport equations for coarse-grained beaches. Coastal Engineering, Vol. 40, 243-275

Vaughan, A., 2001. Shingle bypassing; solving an erosion problem. Papers and proceedings 36th DEFRA (MAFF) conference of river and coastal engineers, UK

Wang, P., Kraus, N.C., and Davis, R.A., 1998. Total longshore transport rate in the surf zone; field measurements and empirical prediction. Journal Coastal Research 14 (1), 2690282

Wang, P. and Kraus, N.C., 1999. Longshore sediment transport rate measured by short-term impoundment. Journal of Waterway, Port, Coastal and Ocean Engineering, Vol. 125, No. 3, 118-126.

Watts, G.M., 1953. A study of sand movement at south Lake Worth Inlet, Florida. Tech. Memorandum 42, Beach Erosion Board, Corps of Engineers, USA